A PRIORI AND A POSTERIORI ERROR ANALYSIS FOR A VORTICITY-BASED MIXED FORMULATION OF THE GENERALIZED STOKES EQUATIONS

VERÓNICA ANAYA[⋆], DAVID MORA[⋆,†], RICARDO OYARZÚA[⋆,†], AND RICARDO RUIZ-BAIER[‡]

Abstract. This paper deals with the analysis of new mixed finite element methods for the generalized Stokes problem formulated in terms of velocity, vorticity and pressure, with non-standard boundary conditions. By employing an extension of the Babuška-Brezzi theory, it is proved that the resulting continuous and discrete variational formulations are well-posed. In particular, on the one hand we show that Raviart-Thomas elements of order $k \geq 0$ for the approximation of the velocity field, piecewise continuous polynomials of degree $k+1$ for the vorticity, and piecewise polynomials of degree k for the pressure, yield unique solvability of the discrete problem. On the other hand, we also show that families of finite elements based on Brezzi-Douglas-Marini elements of order $k+1$ for the approximation of velocity, piecewise continuous polynomials of degree $k+2$ for the vorticity, and piecewise polynomials of degree k for the pressure ensure the well-posedness of the associated Galerkin scheme. We note that these families provide exactly divergence-free approximations of the velocity field. We establish a priori error estimates in the natural norms and we carry out the reliability and efficiency analysis of a residual-based a posteriori error estimator. Finally, we report several numerical experiments illustrating the behavior of the proposed schemes and confirming our theoretical results on unstructured meshes. Additional examples of cases not covered by our theory are also presented.

1. Introduction

This paper is concerned with the numerical study of the generalized Stokes problem, also known as the linear Brinkman problem, differing from the classical Stokes system in the presence of a zeroth order term for the velocity in the momentum equation, and which is usually encountered after time discretizations of transient Stokes, or when considering a fluid in a mixture of porous and viscous regions and therefore ranging from Stokes to Darcy regimes. Our focus will be on the velocity–vorticity–pressure formulation of the mentioned problem.

There exist a great deal of numerical techniques to solve these equations, each one of them with diverse features and, in general, being tested for many fundamental problems and industrial applications including for instance, filtering modeling, subsurface water treatment, oil recovery, and several others. Here, we concentrate on the development of mixed finite element formulations, as e.g. the variational problem in [14], which is recast as a twofold saddle point problem and it is analyzed based on the introduction of the flux and the tensor gradient of the velocity as further unknowns. In that contribution the flux is approximated by lowest order Raviart–Thomas elements, whereas the velocity and pressure fields are approximated by piecewise constant functions. In [31], the pseudostress and the trace-free velocity gradient are introduced as auxiliary unknowns and a pseudostress-velocity formulation is considered,

Date: July 30, 2014.

1991 *Mathematics Subject Classification.* 65N30, 65N12, 76D07, 65N15.

Key words and phrases. Generalized Stokes equations; vorticity-based formulation; mixed finite elements; exactly divergence-free velocity; error analysis.

[⋆]GIMNAP, Departamento de Matemática, Facultad de Ciencias, Universidad del Bío-Bío, Casilla 5-C, Concepción, Chile. Email: {vanaya,dmora,royarzua}@ubiobio.cl.

[†]Centro de Investigación en Ingeniería Matemática (CI^{2}MA), Universidad de Concepción, Casilla 160-C, Concepción, Chile.

[‡]Institut des Sciences de la Terre, Faculté des Géosciences et de l'Environnement, UNIL-Mouline Géopolis, Université de Lausanne, CH-1015 Lausanne, Switzerland. Email: ricardo.ruizbaier@unil.ch.

existence, uniqueness, and error estimates are proposed. In addition, a mixed method associated to a pseudostress based formulation for the Brinkman problem has been introduced and analyzed in [25], in which the main unknown is given by the pseudostress, whereas the velocity and pressure fields are easily recovered through a simple postprocessing procedure.

Special interest lies in the case where the vorticity is introduced as an independent unknown (which is a key field in several applications), since no numerical differentiation of the velocity is needed to compute the additional field, boundary conditions for external flows can be treated in a natural way, and non-inertial effects can be readily included by simply modifying initial and boundary data [36]. Several numerical methods exploit these properties, as for instance, different formulations based on least-squares, stabilization techniques, mixed finite elements, spectral discretizations, and hybridizable discontinuous Galerkin methods (see for instance [2, 3, 7, 10, 12, 21, 16, 17, 19, 20, 24, 33, 34, 35], and the references therein). In this article, we propose a new finite element approximation of the generalized Stokes equations, written in terms of the vorticity, velocity, and pressure fields. A further goal of the present approach is to build different inf-sup stable families of finite elements to approximate the model problem, allowing a direct approximation of the vorticity with optimal accuracy, and without the need of postprocessing. This appears to be quite difficult in mixed methods written only in terms of vector potential-vorticity [20, 29, 30]. In addition, the proposed method exhibits an exactly divergence-free approximation of the velocity, and thus, it exactly preserves an essential constraint of the governing equations.

On the other hand, adaptive mesh refinement strategies based on a posteriori error indicators play a relevant role in the numerical solution of flow problems, and partial differential equations in a general sense. For instance, they guarantee the convergence of finite element solutions, specially in the presence of complex geometries that could eventually lead to spurious solutions [38], and they provide substantial improvements in the accuracy of the approximations for given computational burden [1]. With this in mind, we also introduce a reliable and efficient residual-based a posteriori error estimator for the mixed problem, which can be computed locally, and hence, at a relatively low computational cost.

A priori error estimates have been recently derived for augmented mixed formulations based on vorticity-velocity-pressure variables of the Brinkman equations, including also the axisymmetric case [5, 6]. Moreover, a dual mixed formulation has been introduced and analyzed in [37] for the Brinkman problem. The well-posedness of the continuous and discrete formulations have been carried out using the Babuška theory, and optimal error estimates are proved. In contrast, the proposed variational formulation is analyzed using standard tools in the realm of mixed problems and an a posteriori error estimator has been developed. To do this, we restrict our problem to the space of divergence-free velocities, and apply results from [13],[23],[26], and [27], to prove that the equivalent resulting saddle-point problem is well-posed. For the numerical approximation, we consider first the family of finite elements $\mathbb{RT}_k - \mathbb{P}_{k+1} - \mathbb{P}_k$, $k \geq 0$, i.e., Raviart-Thomas elements of order k for the velocity field, piecewise continuous polynomials of degree $k+1$ for the vorticity, and piecewise polynomials of degree k for the pressure. Since the proposed method provides an exactly divergence-free approximation of the velocity, we prove unique solvability of the discrete problem by adapting the same tools utilized for the continuous problem. In addition, the resulting finite element discretization turns to be convergent with optimal rate of convergence whenever the exact solution of the problem is regular enough. Next, we develop a reliable and efficient residual-based a posteriori error estimator for the proposed formulation. The proof of reliability makes use of the global continuous inf-sup condition of the variational formulation restricted to the space of divergence-free velocities, and the local approximation properties of the Clément and Raviart-Thomas operators, whereas for the efficiency we utilize inverse inequalities, and the localization technique based on element-bubble and edge-bubble functions. Moreover, numerical experiments with the family of finite elements considered in this paper perform satisfactorily for a variety of boundary conditions. We also introduce and comment the applicability of the present framework using other families of finite elements, as for instance Brezzi-Douglas-Marini elements of order $k+1$ for the velocity field, piecewise continuous polynomials of degree $k+2$ for the vorticity, and piecewise polynomials of degree k for the pressure. Finally, we stress that the

proposed methodology can be used to analyze the extension to the three-dimensional case, and to study a larger class of problems, including the coupling with Darcy flows or with transport phenomena.

Outline. The remainder of the paper has been structured as follows. In what is left from this section, we introduce some standard notation, required functional spaces, and we describe the boundary value problem of interest. Section 2 presents the associate variational formulation, it provides an abstract framework where our formulation lies, and then we prove its unique solvability along with some stability properties. In Section 3, we present two mixed finite element schemes and we provide a stability result and obtain error estimates for the proposed methods. The derivation and analysis of a reliable and efficient residual-based a posteriori error estimator for this problem is carried out in Section 4. Several numerical results illustrating the convergence behavior predicted by the theory and allowing us to assess the performance of the methods are collected in Section 5, and we close with some final remarks in Section 6.

Preliminaries. We will denote a simply connected polygonal Lipschitz bounded domain of $\mathbb{R}^2$ by Ω and $\boldsymbol{n} = (n_i)_{1\le i\le 2}$ is the outward unit normal vector to the boundary $\partial\Omega$. The vector $\boldsymbol{t} = (t_i)_{1\le i\le 2}$ is the unit tangent to $\partial\Omega$ oriented such that $t_1 = -n_2$, $t_2 = n_1$. Moreover, we assume that $\partial\Omega$ admits a disjoint partition $\partial\Omega = \Gamma\cup\Sigma$. For the sake of simplicity, we also assume that both Γ and Σ have positive measure. For any $s \ge 0$, the notation $\|\cdot\|_{s,\Omega}$ stands for the norm of the Hilbertian Sobolev spaces $\mathrm{H}^s(\Omega)$ or $\mathrm{H}^s(\Omega)^2$, with the usual convention $\mathrm{H}^0(\Omega) := \mathrm{L}^2(\Omega)$. For $s \ge 0$, we recall the definition of the Hilbert space

$$\mathrm{H}^s(\mathrm{div};\Omega) := \{\boldsymbol{v} \in \mathrm{H}^s(\Omega)^n : \ \mathrm{div}\,\boldsymbol{v} \in \mathrm{H}^s(\Omega)\},$$

endowed with the norm $\|\boldsymbol{v}\|^2_{\mathrm{H}^s(\mathrm{div};\Omega)} := \|\boldsymbol{v}\|^2_{s,\Omega} + \|\mathrm{div}\,\boldsymbol{v}\|^2_{s,\Omega}$. We will denote $\mathrm{H}(\mathrm{div};\Omega) := \mathrm{H}^0(\mathrm{div};\Omega)$.

Moreover, c and C, with or without subscripts, tildes, or hats, will represent a generic constant independent of the mesh parameter h, assuming different values in different occurrences. In addition, for any vector field $\boldsymbol{v} = (v_i)_{i=1,2}$ and any scalar field θ we recall the differential operators:

$$\mathrm{div}\,\boldsymbol{v} := \partial_1 v_1 + \partial_2 v_2, \quad \mathrm{rot}\,\boldsymbol{v} := \partial_1 v_2 - \partial_2 v_1, \quad \nabla\theta := \begin{pmatrix}\partial_1\theta\\ \partial_2\theta\end{pmatrix}, \quad \mathbf{curl}\,\theta := \begin{pmatrix}\partial_2\theta\\ -\partial_1\theta\end{pmatrix}.$$

The model problem. We are interested in the generalized Stokes problem [30], formulated in terms of the velocity $\boldsymbol{u}$, the vorticity ω and the pressure p of an incompressible viscous fluid: Given a force density $\boldsymbol{f}$, vector fields $\boldsymbol{a}$ and $\boldsymbol{b}$, and scalar fields p_0 and ω_0, we seek a vector field $\boldsymbol{u}$, a scalar field ω, and a scalar field p such that

$$\begin{aligned}
\sigma\boldsymbol{u} + \nu\,\mathbf{curl}\,\omega + \nabla p &= \boldsymbol{f} && \text{in } \Omega,\\
\omega - \mathrm{rot}\,\boldsymbol{u} &= 0 && \text{in } \Omega,\\
\mathrm{div}\,\boldsymbol{u} &= 0 && \text{in } \Omega,\\
\boldsymbol{u}\cdot\boldsymbol{t} &= \boldsymbol{a}\cdot\boldsymbol{t} && \text{on } \Sigma,\\
p &= p_0 && \text{on } \Sigma,\\
\boldsymbol{u}\cdot\boldsymbol{n} &= \boldsymbol{b}\cdot\boldsymbol{n} && \text{on } \Gamma,\\
\omega &= \omega_0 && \text{on } \Gamma,
\end{aligned} \tag{1.1}$$

where $\boldsymbol{u}\cdot\boldsymbol{t}$ and $\boldsymbol{u}\cdot\boldsymbol{n}$ stand for the normal and the tangential components of the velocity, respectively. In the model, $\nu > 0$ is the kinematic viscosity of the fluid and $\sigma > 0$ is a parameter proportional to the inverse of the time-step.

In addition, we assume that a *boundary compatibility condition* holds, i.e., there exists a velocity field $\boldsymbol{w} \in \mathrm{L}^2(\Omega)^2$ satisfying $\mathrm{div}\,\boldsymbol{w} = 0$ a.e. in Ω, $\boldsymbol{w}\cdot\boldsymbol{t} = \boldsymbol{a}\cdot\boldsymbol{t}$ on Σ, and $\boldsymbol{w}\cdot\boldsymbol{n} = \boldsymbol{b}\cdot\boldsymbol{n}$ on Γ. For a detailed study on different types of standard and non-standard boundary conditions for incompressible flows, we refer to [11]. We observe that the boundary conditions considered here are relevant in the context of e.g. geophysical fluids and shallow water models [32].

For the sake of simplicity, we will work with homogeneous boundary conditions for the normal velocity and, subsequently, for the vorticity, i.e., $\boldsymbol{b} = \mathbf{0}$ and $\omega_0 = 0$ on Γ. Nevertheless, these restrictions do not affect the generality of the forthcoming analysis.

2. A mixed velocity-vorticity-pressure formulation

2.1. **Variational formulation and preliminary results.** In this section, we propose a mixed variational formulation of system (1.1). First, we need to introduce the following spaces that we will consider in the sequel:

$$\mathrm{H} := \{\boldsymbol{v} \in \mathrm{H}(\mathrm{div};\Omega) : \boldsymbol{v}\cdot\boldsymbol{n} = 0 \text{ on } \Gamma\}, \quad \mathrm{Z} := \{\theta \in \mathrm{H}^1(\Omega) : \theta = 0 \text{ on } \Gamma\}, \quad \text{and} \quad \mathrm{Q} := \mathrm{L}^2(\Omega).$$

We endow each space with its natural norm. Moreover, the symbol $\langle\cdot,\cdot\rangle_\Sigma$ will denote the duality pairing between $\mathrm{H}^{-1/2}(\Sigma)$ and $\mathrm{H}^{1/2}(\Sigma)$ with respect to the $\mathrm{L}^2(\Sigma)$-inner product.

Now, by testing system (1.1) with adequate functions and imposing the boundary conditions, we end up with the following mixed variational formulation:

Find $(\boldsymbol{u},\omega,p) \in \mathrm{H}\times\mathrm{Z}\times\mathrm{Q}$ *such that*

$$\begin{aligned}
\sigma\int_\Omega \boldsymbol{u}\cdot\boldsymbol{v} + \nu\int_\Omega \mathbf{curl}\,\omega\cdot\boldsymbol{v} - \int_\Omega p\,\mathrm{div}\,\boldsymbol{v} &= \int_\Omega \boldsymbol{f}\cdot\boldsymbol{v} - \langle \boldsymbol{v}\cdot\boldsymbol{n}, p_0\rangle_\Sigma && \forall \boldsymbol{v}\in\mathrm{H},\\
\nu\int_\Omega \mathbf{curl}\,\theta\cdot\boldsymbol{u} - \nu\int_\Omega \omega\theta &= -\nu\langle \boldsymbol{a}\cdot\boldsymbol{t},\theta\rangle_\Sigma && \forall \theta\in\mathrm{Z},\\
-\int_\Omega q\,\mathrm{div}\,\boldsymbol{u} &= 0 && \forall q\in\mathrm{Q}.
\end{aligned}$$

This variational problem can be rewritten as follows: *Find* $(\boldsymbol{u},\omega,p) \in \mathrm{H}\times\mathrm{Z}\times\mathrm{Q}$ *such that*

$$\begin{aligned}
a(\boldsymbol{u},\boldsymbol{v}) + b_1(\boldsymbol{v},\omega) + b_2(\boldsymbol{v},p) &= G(\boldsymbol{v}) && \forall \boldsymbol{v}\in\mathrm{H},\\
b_1(\boldsymbol{u},\theta) - d(\omega,\theta) &= F(\theta) && \forall \theta\in\mathrm{Z},\\
b_2(\boldsymbol{u},q) &= 0 && \forall q\in\mathrm{Q},
\end{aligned} \tag{2.1}$$

where the bilinear forms $a : \mathrm{H}\times\mathrm{H}\to\mathbb{R}$, $b_1 : \mathrm{H}\times\mathrm{Z}\to\mathbb{R}$, $d : \mathrm{Z}\times\mathrm{Z}\to\mathbb{R}$, $b_2 : \mathrm{H}\times\mathrm{Q}\to\mathbb{R}$, and the linear functionals $G : \mathrm{H}\to\mathbb{R}$, and $F : \mathrm{Z}\to\mathbb{R}$ are defined by

$$\begin{aligned}
a(\boldsymbol{u},\boldsymbol{v}) &:= \sigma\int_\Omega \boldsymbol{u}\cdot\boldsymbol{v}, \quad b_1(\boldsymbol{v},\theta) := \nu\int_\Omega \mathbf{curl}\,\theta\cdot\boldsymbol{v},\\
d(\omega,\theta) &:= \nu\int_\Omega \omega\theta, \quad b_2(\boldsymbol{v},q) := -\int_\Omega q\,\mathrm{div}\,\boldsymbol{v},\\
G(\boldsymbol{v}) &:= \int_\Omega \boldsymbol{f}\cdot\boldsymbol{v} - \langle \boldsymbol{v}\cdot\boldsymbol{n}, p_0\rangle_\Sigma, \qquad F(\theta) := -\nu\langle \boldsymbol{a}\cdot\boldsymbol{t},\theta\rangle_\Sigma,
\end{aligned}$$

for all $\boldsymbol{u},\boldsymbol{v}\in\mathrm{H}$, $\omega,\theta\in\mathrm{Z}$, and $q\in\mathrm{Q}$.

In order to analyze the variational formulation (2.1), let us consider the Kernel of $b_2(\cdot,\cdot)$

$$\mathrm{X} := \{\boldsymbol{v}\in\mathrm{H} \,:\, b_2(\boldsymbol{v},q) = 0, \quad \forall\, q\in Q\} \,=\, \{\boldsymbol{v}\in\mathrm{H} \,:\, \mathrm{div}\,\boldsymbol{v} \,=\, 0\},$$

and let us recall that the bilinear form b_2 satisfies the inf-sup condition:

$$\sup_{\substack{\boldsymbol{v}\in\mathrm{H}\\ \boldsymbol{v}\neq 0}} \frac{|b_2(\boldsymbol{v},q)|}{\|\boldsymbol{v}\|_{\mathrm{H}(\mathrm{div};\Omega)}} \geq \beta_2\|q\|_{0,\Omega} \quad \forall q\in\mathrm{Q}, \tag{2.2}$$

with an inf-sup constant $\beta_2 > 0$ only depending on Ω; see [23], for instance.

A proof of the following auxiliary abstract result can be found in [27, Lemma 3.4] (see also [26, Lemma 2.1] for a nonlinear version of it).

Lemma 2.1. *Let $(\mathcal{X}, \langle\cdot,\cdot\rangle_{\mathcal{X}})$ and $(\mathcal{Y}, \langle\cdot,\cdot\rangle_{\mathcal{Y}})$ be Hilbert spaces. Let $\mathcal{A} : \mathcal{X}\times\mathcal{X} \to \mathbb{R}$, $\mathcal{B} : \mathcal{X}\times\mathcal{Y} \to \mathbb{R}$, and $\mathcal{D} : \mathcal{Y}\times\mathcal{Y} \to \mathbb{R}$ be bounded bilinear forms, and let $\mathcal{G} : \mathcal{X} \to \mathbb{R}$ and $\mathcal{F} : \mathcal{Y} \to \mathbb{R}$ be bounded functionals. Assume that*

i) *there exists $\bar{\alpha} > 0$ such that $\mathcal{A}(x,x) \geq \bar{\alpha}\,\|x\|^2_{\mathcal{X}} \quad \forall\, x \in \mathcal{X}$,*

ii) *there exists $\bar{\beta} > 0$ such that $\displaystyle\sup_{\substack{x\in\mathcal{X}\\ x\neq 0}} \frac{\mathcal{B}(x,y)}{\|x\|_{\mathcal{X}}} \geq \bar{\beta}\,\|y\|_{\mathcal{Y}} \quad \forall\, y \in \mathcal{Y}$,*

iii) *$\mathcal{D}(y,y) \geq 0 \quad \forall\, y \in \mathcal{Y}$.*

Then, there exists a unique $(x,y) \in \mathcal{X}\times\mathcal{Y}$, such that

$$\begin{aligned} \mathcal{A}(x,r) + \mathcal{B}(r,y) &= \mathcal{G}(r) \quad \forall\, r \in \mathcal{X},\\ \mathcal{B}(x,v) - \mathcal{D}(y,v) &= \mathcal{F}(v) \quad \forall\, v \in \mathcal{Y}. \end{aligned} \tag{2.3}$$

Moreover, there exists $C > 0$, independent of the solution, such that

$$\|x\|_{\mathcal{X}} + \|y\|_{\mathcal{Y}} \leq C(\|\mathcal{G}\|_{\mathcal{X}'} + \|\mathcal{F}\|_{\mathcal{Y}'}).$$

2.2. **Analysis of the continuous formulation.** In this section, we prove that the continuous variational formulation (2.1) is well-posed. To that end, it is enough to study the reduced counterpart of (2.1) defined on $\mathrm{X}\times\mathrm{Z}$: Find $(\boldsymbol{u},\omega) \in \mathrm{X}\times\mathrm{Z}$ such that

$$\begin{aligned} a(\boldsymbol{u},\boldsymbol{v}) + b_1(\boldsymbol{v},\omega) &= G(\boldsymbol{v}) \qquad \forall \boldsymbol{v} \in \mathrm{X},\\ b_1(\boldsymbol{u},\theta) - d(\omega,\theta) &= F(\theta) \qquad \forall \theta \in \mathrm{Z}. \end{aligned} \tag{2.4}$$

In fact, the following result establishes the equivalence between (2.1) and (2.4).

Lemma 2.2. *If $(\boldsymbol{u},\omega,p) \in \mathrm{H}\times\mathrm{Z}\times\mathrm{Q}$ is a solution of (2.1), then $\boldsymbol{u} \in \mathrm{X}$, and $(\boldsymbol{u},\omega) \in \mathrm{X}\times\mathrm{Z}$ is also a solution of (2.4). Conversely, if $(\boldsymbol{u},\omega) \in \mathrm{X}\times\mathrm{Z}$ is a solution of (2.4), then there exists a unique pressure $p \in \mathrm{Q}$ such that $(\boldsymbol{u},\omega,p) \in \mathrm{H}\times\mathrm{Z}\times\mathrm{Q}$ is a solution of (2.1).*

Proof. The proof follows basically from the inf-sup condition (2.2). We omit further details and refer to [30]. □

According to the above, we will now turn to prove that the continuous variational formulation (2.4) is well-posed.

Theorem 2.1. *The variational problem (2.4) admits a unique solution $(\boldsymbol{u},\omega) \in \mathrm{X}\times\mathrm{Z}$. Moreover, there exists $C > 0$ such that*

$$\|\boldsymbol{u}\|_{\mathrm{H(div;\Omega)}} + \|\omega\|_{1,\Omega} \leq C(\|\boldsymbol{f}\|_{0,\Omega} + \|p_0\|_{1/2,\Sigma} + \|\boldsymbol{a}\cdot\boldsymbol{t}\|_{-1/2,\Sigma}). \tag{2.5}$$

Proof. It suffices to verify the hypotheses of Lemma 2.1. First, we note that the bilinear forms $a(\cdot,\cdot)$, $b_1(\cdot,\cdot)$, and $d(\cdot,\cdot)$ are bounded. Furthermore, it is easy to see that the bilinear forms a and d satisfy i) and iii), respectively.

The next step consists in proving that the bilinear form $b_1(\cdot,\cdot)$ satisfies hypothesis ii). In fact, given $\theta \in \mathrm{Z}$, we let $\tilde{\boldsymbol{v}} := \mathbf{curl}\,\theta$, hence $\tilde{\boldsymbol{v}} \in \mathrm{X}$. Then, using the Poincaré inequality, we obtain

$$\sup_{\substack{\boldsymbol{v}\in\mathrm{X}\\ \boldsymbol{v}\neq 0}} \frac{b_1(\boldsymbol{v},\theta)}{\|\boldsymbol{v}\|_{\mathrm{H(div;\Omega)}}} \geq \frac{b_1(\tilde{\boldsymbol{v}},\theta)}{\|\tilde{\boldsymbol{v}}\|_{0,\Omega}} = |\theta|_{1,\Omega} \geq C\|\theta\|_{1,\Omega} \quad \forall \theta \in \mathrm{Z},$$

which finishes the proof. □

The following result establishes the corresponding stability estimate for the pressure.

Corollary 2.1. *Let $(\boldsymbol{u},\omega)\in \mathrm{X}\times\mathrm{Z}$, be the unique solution of (2.4), with $\boldsymbol{u}$ and ω satisfying (2.5). In addition, let $p\in Q$ be the unique pressure provided by Lemma 2.2, so that $(\boldsymbol{u},\omega,p)\in \mathrm{H}\times\mathrm{Z}\times\mathrm{Q}$ is the unique solution of (2.1). Then, there exits $C>0$, independent of the solution, such that*

$$\|p\|_{0,\Omega}\leq C(\|\boldsymbol{f}\|_{0,\Omega}+\|p_0\|_{1/2,\Sigma}+\|\boldsymbol{a}\cdot\boldsymbol{t}\|_{-1/2,\Sigma}).$$

Proof. From the inf-sup condition (2.2), and the first equation of (2.1), we obtain

$$\|p\|_{0,\Omega}\leq\frac{1}{\beta_2}\sup_{\substack{\boldsymbol{v}\in\mathrm{H}\\ \boldsymbol{v}\neq 0}}\frac{|b_2(\boldsymbol{v},p)|}{\|\boldsymbol{v}\|_{\mathrm{H}(\mathrm{div};\Omega)}}=\frac{1}{\beta_2}\sup_{\substack{\boldsymbol{v}\in\mathrm{H}\\ \boldsymbol{v}\neq 0}}\frac{|G(\boldsymbol{v})-a(\boldsymbol{u},\boldsymbol{v})-b_1(\boldsymbol{v},\omega)|}{\|\boldsymbol{v}\|_{\mathrm{H}(\mathrm{div};\Omega)}},$$

which together to (2.5), and the boundedness of G, a and b_1, complete the proof. □

We end this section with the converse derivation of problem (2.1). More precisely, the following theorem establishes that the unique solution of (2.1) solves the original problem described in (1.1). This result will be used later on in Section 4.2 to prove the efficiency of our a posteriori error estimator.

Theorem 2.2. *Let $(\boldsymbol{u},\omega,p)\in\mathrm{H}\times\mathrm{Z}\times\mathrm{Q}$ the unique solution of (2.1). Then $\sigma\boldsymbol{u}+\nu\,\mathbf{curl}\,\omega+\nabla p=\boldsymbol{f}$ in Ω, $\omega-\mathrm{rot}\,\boldsymbol{u}=0$ in Ω, $\mathrm{div}\,\boldsymbol{u}=0$ in Ω, $\boldsymbol{u}\in\mathrm{H}^1(\Omega)^2$, $p\in\mathrm{H}^1(\Omega)$, and $\boldsymbol{u}$, ω, and p satisfy the boundary conditions described in (1.1).*

Proof. It basically follows by applying integration by parts backwardly in (2.1) and using suitable test functions. Further details are omitted. □

3. Mixed finite element schemes

In this section, we will construct two mixed finite element schemes associated to (2.1), we define explicit finite element subspaces yielding the unique solvability of the discrete schemes, derive the a priori error estimates, and provide the rate of convergence of the methods.

Let $\mathcal{T}_h$ be a regular family of triangulations of the polygonal region $\bar{\Omega}$ by triangles T of diameter h_T with mesh size $h:=\max\{h_T:T\in\mathcal{T}_h\}$, and such that there holds $\bar{\Omega}=\cup\{T:T\in\mathcal{T}_h\}$. In addition, given an integer $k\geq 0$ and a subset S of $\mathbb{R}^2$, we denote by $\mathbb{P}_k(S)$ the space of polynomials in two variables defined in S of total degree at most k.

Let us introduce the local Raviart-Thomas space of order k

$$\mathbb{RT}_k(T):=\mathbb{P}_k(T)^2\oplus\mathbb{P}_k(T)\boldsymbol{x},$$

where $\boldsymbol{x}$ is a generic vector of $\mathbb{R}^2$, and let us define the following finite element subspaces:

$$\mathrm{H}_h:=\{\boldsymbol{v}_h\in\mathrm{H}:\boldsymbol{v}_h|_T\in\mathbb{RT}_k(T),\ \forall T\in\mathcal{T}_h\},\tag{3.1}$$

$$\mathrm{Z}_h:=\{\theta_h\in\mathrm{Z}:\theta_h|_T\in\mathbb{P}_{k+1}(T),\ \forall T\in\mathcal{T}_h\},\tag{3.2}$$

$$\mathrm{Q}_h:=\{q_h\in\mathrm{Q}:q_h|_T\in\mathbb{P}_k(T),\ \forall T\in\mathcal{T}_h\}.\tag{3.3}$$

Then, the Galerkin scheme associated with the continuous variational formulation (2.1) reads as follows: *Find $(\boldsymbol{u}_h,\omega_h,p_h)\in\mathrm{H}_h\times\mathrm{Z}_h\times\mathrm{Q}_h$ such that*

$$\begin{aligned}
a(\boldsymbol{u}_h,\boldsymbol{v}_h)+b_1(\boldsymbol{v}_h,\omega_h)+b_2(\boldsymbol{v}_h,p_h)&=G(\boldsymbol{v}_h) && \forall\boldsymbol{v}_h\in\mathrm{H}_h,\\
b_1(\boldsymbol{u}_h,\theta_h)-d(\omega_h,\theta_h)&=F(\theta_h) && \forall\theta_h\in\mathrm{Z}_h,\\
b_2(\boldsymbol{u}_h,q_h)&=0 && \forall q_h\in\mathrm{Q}_h.
\end{aligned}\tag{3.4}$$

One of the key features of the scheme proposed in (3.4), besides the direct approximation of the vorticity, is that the approximate velocity $\boldsymbol{u}_h$ is exactly divergence-free in Ω. To discuss this property, we introduce the discrete kernel of b_2:

$$\mathrm{X}_h:=\{\boldsymbol{v}_h\in\mathrm{H}_h\ :\ b_2(\boldsymbol{v}_h,q_h)=0,\quad\forall\,q\in\mathrm{Q}_h\}.$$

Since $\operatorname{div} \mathrm{H}_h \subseteq \mathrm{Q}_h$, it can be readily seen that

$$\mathrm{X}_h := \{\boldsymbol{v}_h \in \mathrm{H}_h \,:\, \operatorname{div} \boldsymbol{v}_h \equiv 0 \quad \text{in} \quad \Omega\}. \tag{3.5}$$

Let us observe now that, similarly to the continuous case, the bilinear form b_2 satisfies the discrete inf-sup condition

$$\sup_{\substack{\boldsymbol{v}_h \in \mathrm{H}_h \\ \boldsymbol{v}_h \neq 0}} \frac{b_2(\boldsymbol{v}_h, q_h)}{\|\boldsymbol{v}_h\|_{\mathrm{H}(\mathrm{div};\Omega)}} \geq \tilde{\beta}_2 \|q_h\|_{0,\Omega} \quad \forall q_h \in \mathrm{Q}_h, \tag{3.6}$$

with the inf-sup constant $\tilde{\beta}_2$ independent of discretization parameter h; see [23] for instance.

Throughout the rest of this section, we will show that the discrete variational formulation (3.4) is well-posed and that it satisfies the corresponding Céa estimate. In order to do this, we proceed as in Section 2.2, and introduce the following reduced version of (3.4) on the product space $\mathrm{X}_h \times \mathrm{Z}_h$: Find $(\boldsymbol{u}_h, \omega_h) \in \mathrm{X}_h \times \mathrm{Z}_h$ such that

$$\begin{aligned} a(\boldsymbol{u}_h, \boldsymbol{v}_h) + b_1(\boldsymbol{v}_h, \omega_h) &= G(\boldsymbol{v}_h) \qquad \forall\, \boldsymbol{v}_h \in \mathrm{X}_h, \\ b_1(\boldsymbol{u}_h, \theta_h) - d(\omega_h, \theta_h) &= F(\theta_h) \qquad \forall\, \theta_h \in \mathrm{Z}_h. \end{aligned} \tag{3.7}$$

The following result establishes the equivalence between (3.4) and (3.7), which is a direct consequence of the inf-sup condition (3.6).

Lemma 3.1. *If $(\boldsymbol{u}_h, \omega_h, p_h) \in \mathrm{H}_h \times \mathrm{Z}_h \times \mathrm{Q}_h$ is a solution of (3.4), then $\boldsymbol{u}_h \in \mathrm{X}_h$, and $(\boldsymbol{u}_h, \omega_h) \in \mathrm{X}_h \times \mathrm{Z}_h$ is also a solution of (3.7). Conversely, if $(\boldsymbol{u}_h, \omega_h) \in \mathrm{X}_h \times \mathrm{Z}_h$ is a solution of (3.7), then there exists a unique pressure $p_h \in \mathrm{Q}_h$ such that $(\boldsymbol{u}_h, \omega_h, p_h) \in \mathrm{H}_h \times \mathrm{Z}_h \times \mathrm{Q}_h$ is a solution of (3.4).*

According to the above, in what follows we will focus on analyzing problem (3.7). To this end, let us first collect some previous results and notations to be used in the sequel. We start by introducing the discrete version of Lemma 2.1.

Lemma 3.2. *Let $(\mathcal{X}, \langle\cdot,\cdot\rangle_{\mathcal{X}})$ and $(\mathcal{Y}, \langle\cdot,\cdot\rangle_{\mathcal{Y}})$ be Hilbert spaces and let $\{\mathcal{X}_h\}_{h>0}$ and $\{\mathcal{Y}_h\}_{h>0}$ be a sequence of finite-dimensional subspaces of $\mathcal{X}$ and $\mathcal{Y}$, respectively. Let $\mathcal{A} : \mathcal{X} \times \mathcal{X} \to \mathbb{R}$, $\mathcal{B} : \mathcal{X} \times \mathcal{Y} \to \mathbb{R}$, and $\mathcal{D} : \mathcal{Y} \times \mathcal{Y} \to \mathbb{R}$ be bounded bilinear forms, and let $\mathcal{G} : \mathcal{X} \to \mathbb{R}$ and $\mathcal{F} : \mathcal{Y} \to \mathbb{R}$ be bounded functionals. Assume that $\mathcal{A}$ and $\mathcal{D}$ satisfy* i) *and* iii) *in Lemma 2.1, respectively. In addition, assume that there exists $\bar{\beta}_h > 0$, independent of the discretization parameter h, such that*

$$\sup_{\substack{x_h \in \mathcal{X}_h \\ x_h \neq 0}} \frac{\mathcal{B}(x_h, y_h)}{\|x_h\|_{\mathcal{X}}} \geq \bar{\beta}_h \, \|y_h\|_{\mathcal{Y}} \quad \forall\, y_h \in \mathcal{Y}_h.$$

Then, there exists a unique $(x_h, y_h) \in \mathcal{X}_h \times \mathcal{Y}_h$, such that

$$\begin{aligned} \mathcal{A}(x_h, r_h) + \mathcal{B}(r_h, y_h) &= \mathcal{G}(r_h) \quad \forall\, r_h \in \mathcal{X}_h, \\ \mathcal{B}(x_h, v_h) - \mathcal{D}(y_h, v_h) &= \mathcal{F}(v_h) \quad \forall\, v_h \in \mathcal{Y}_h. \end{aligned} \tag{3.8}$$

Moreover, there exist positive constants C_1, $C_2 > 0$, independent of the discretization parameter h, such that

$$\|x_h\|_{\mathcal{X}} + \|y_h\|_{\mathcal{Y}} \leq C_1 (\|\mathcal{G}|_{\mathcal{X}_h}\|_{\mathcal{X}_h'} + \|\mathcal{F}|_{\mathcal{Y}_h}\|_{\mathcal{Y}_h'}),$$

and

$$\|x - x_h\|_{\mathcal{X}} + \|y - y_h\|_{\mathcal{Y}} \leq C_2 \inf_{(z_h, s_h) \in \mathcal{X}_h \times \mathcal{Y}_h} (\|x - z_h\|_{\mathcal{X}} + \|y - s_h\|_{\mathcal{Y}}),$$

where $(x, y) \in \mathcal{X} \times \mathcal{Y}$ is the unique solution of problem (2.3).

Proof. Unique solvability and stability of (3.8) follow analogously to the continuous case (see again [26] for details), whereas the corresponding Céa's estimate follows by applying standard arguments such as the Galerkin orthogonality property. We omit further details and refer to [23] and [13]. □

We now introduce the Raviart-Thomas interpolation operator [13] $\mathcal{R} : \mathrm{H}^s(\Omega)^2 \cap \mathrm{H} \to \mathrm{H}_h$ for all $s > 0$, for which we review some properties to be used in the sequel: There exists $C > 0$, independent of h, such that for all $s \in (0, k+1]$:

$$\|\boldsymbol{v} - \mathcal{R}\boldsymbol{v}\|_{\mathrm{H}(\mathrm{div};\Omega)} \leq Ch^s \|\boldsymbol{v}\|_{\mathrm{H}^s(\mathrm{div};\Omega)} \quad \forall \boldsymbol{v} \in \mathrm{H}^s(\mathrm{div};\Omega) \cap \mathrm{H}. \tag{3.9}$$

Now, for all $s > 0$, let $\Pi : \mathrm{H}^{1+s}(\Omega) \to \mathrm{Z}_h$ be the usual Lagrange interpolant. This operator satisfies the following error estimate: There exists $C > 0$, independent of h, such that for all $s \in (0, k+1]$:

$$\|\theta - \Pi\theta\|_{1,\Omega} \leq Ch^s \|\theta\|_{1+s,\Omega} \quad \forall \theta \in \mathrm{H}^{1+s}(\Omega). \tag{3.10}$$

Let $\mathcal{P}$ be the orthogonal projection from $\mathrm{L}^2(\Omega)$ onto the finite element subspace Q_h. We have that $\mathcal{P}$ satisfies the following error estimate for all $s \in (0, k+1]$:

$$\|q - \mathcal{P}q\|_{0,\Omega} \leq Ch^s \|q\|_{s,\Omega} \quad \forall q \in \mathrm{H}^s(\Omega). \tag{3.11}$$

Moreover, the following commuting diagram property holds true:

$$\mathrm{div}\, \mathcal{R}\boldsymbol{v} = \mathcal{P}(\mathrm{div}\, \boldsymbol{v}) \quad \forall \boldsymbol{v} \in \mathrm{H}^s(\Omega)^2 \cap \mathrm{H}(\mathrm{div};\Omega).$$

We are now in a position of establishing the unique solvability and convergence of the reduced discrete problem (3.7).

Theorem 3.1. *Let k be a non-negative integer and let X_h and Z_h be given by (3.5) and (3.2), respectively. Then, there exists a unique $(\boldsymbol{u}_h, \omega_h) \in \mathrm{X}_h \times \mathrm{Z}_h$ solution of the Galerkin scheme (3.7). Moreover, there exist positive constants $\hat{C}_1$, $\hat{C}_2 > 0$ independent of h such that*

$$\|\boldsymbol{u}_h\|_{\mathrm{H}(\mathrm{div};\Omega)} + \|\omega_h\|_{1,\Omega} \leq \hat{C}_1(\|\boldsymbol{f}\|_{0,\Omega} + \|p_0\|_{1/2,\Sigma} + \|\boldsymbol{a}\cdot\boldsymbol{t}\|_{-1/2,\Sigma}), \tag{3.12}$$

and

$$\|\boldsymbol{u} - \boldsymbol{u}_h\|_{\mathrm{H}(\mathrm{div};\Omega)} + \|\omega - \omega_h\|_{1,\Omega} \leq \hat{C}_2 \inf_{(\boldsymbol{v}_h,\theta_h)\in \mathrm{X}_h\times\mathrm{Z}_h} (\|\boldsymbol{u} - \boldsymbol{v}_h\|_{\mathrm{H}(\mathrm{div};\Omega)} + \|\omega - \theta_h\|_{1,\Omega}), \tag{3.13}$$

where $(\boldsymbol{u}, \omega) \in \mathrm{X} \times \mathrm{Z}$ is the unique solution to variational problem (2.4).

Proof. It is enough to verify hypotheses of Lemma 3.2. In fact, since our method is conforming, the bilinear forms $a(\cdot,\cdot)$ and $c(\cdot,\cdot)$ satisfy hypotheses i) and iii) in Lemma 2.1. Next, given $\theta_h \in \mathrm{Z}_h$, we let $\tilde{\boldsymbol{v}}_h := \mathbf{curl}\, \theta_h$, and proceed as in the proof of Theorem 2.1 to obtain

$$\sup_{\substack{\boldsymbol{v}_h\in\mathrm{X}_h\\ \boldsymbol{v}_h\neq 0}} \frac{b_1(\boldsymbol{v}_h,\theta_h)}{\|\boldsymbol{v}_h\|_{\mathrm{H}(\mathrm{div};\Omega)}} \geq \frac{b_1(\tilde{\boldsymbol{v}}_h,\theta_h)}{\|\tilde{\boldsymbol{v}}_h\|_{0,\Omega}} = |\theta_h|_{1,\Omega} \geq C\|\theta_h\|_{1,\Omega} \quad \forall \theta_h \in \mathrm{Z}_h,$$

which completes the proof. □

We now establish the corresponding stability estimate for the discrete pressure and its approximation property.

Corollary 3.1. *Let $(\boldsymbol{u}_h, \omega_h) \in \mathrm{X}_h \times \mathrm{Z}_h$, be the unique solution of (3.7), with $\boldsymbol{u}_h$ and ω_h satisfying (3.12). In addition, let $p_h \in Q_h$ be the unique discrete pressure provided by Lemma 3.1, so that $(\boldsymbol{u}_h, \omega_h, p_h) \in \mathrm{H}_h \times \mathrm{Z}_h \times \mathrm{Q}_h$ is the unique solution of (3.4). Then, there exist positive constants $\bar{C}_1$, $\bar{C}_2 > 0$, independent of h, such that*

$$\|p_h\|_{0,\Omega} \leq \bar{C}_1(\|\boldsymbol{f}\|_{0,\Omega} + \|p_0\|_{1/2,\Sigma} + \|\boldsymbol{a}\cdot\boldsymbol{t}\|_{-1/2,\Sigma}), \tag{3.14}$$

and

$$\|p - p_h\|_{0,\Omega} \leq \bar{C}_2 \inf_{(\boldsymbol{v}_h,\theta_h,q_h)\in \mathrm{H}_h\times\mathrm{Z}_h\times Q_h} (\|\boldsymbol{u} - \boldsymbol{v}_h\|_{\mathrm{H}(\mathrm{div};\Omega)} + \|\omega - \theta_h\|_{1,\Omega} + \|p - q_h\|_{0,\Omega}). \tag{3.15}$$

Proof. Proceeding as in the proof of Corollary 3.1, we observe that from the inf-sup condition (3.6), and the first equation of (3.4), there holds

$$\|p_h\|_{0,\Omega} \leq \frac{1}{\tilde{\beta}_2} \sup_{\substack{\boldsymbol{v}_h \in \mathrm{H}_h \\ \boldsymbol{v}_h \neq 0}} \frac{|b_2(\boldsymbol{v}_h, p_h)|}{\|\boldsymbol{v}_h\|_{\mathrm{H}(\mathrm{div};\Omega)}} = \frac{1}{\tilde{\beta}_2} \sup_{\substack{\boldsymbol{v}_h \in \mathrm{H}_h \\ \boldsymbol{v}_h \neq 0}} \frac{|G(\boldsymbol{v}_h) - a(\boldsymbol{u}_h, \boldsymbol{v}_h) - b_1(\boldsymbol{v}_h, \omega_h)|}{\|\boldsymbol{v}_h\|_{\mathrm{H}(\mathrm{div};\Omega)}},$$

which together to (3.12), and the boundedness of G, a and b_1, yield (3.14).

Next, given $q_h \in \mathrm{Q}_h$, from the first equation of (3.4) and the Galerkin orthogonality result, it follows that

$$b_2(\boldsymbol{v}_h, p_h - q_h) = a(\boldsymbol{u} - \boldsymbol{u}_h, \boldsymbol{v}_h) + b_1(\boldsymbol{v}_h, \omega - \omega_h) + b_2(\boldsymbol{v}_h, p - q_h) \quad \forall\, \boldsymbol{v}_h \in \mathrm{H}_h.$$

Then, applying again the inf-sup condition (3.6) and the boundedness of a, b_1 and b_2, we obtain

$$\begin{aligned} \|p_h - q_h\|_{0,\Omega} \leq & \frac{1}{\tilde{\beta}_2} \sup_{\substack{\boldsymbol{v}_h \in \mathrm{H}_h \\ \boldsymbol{v}_h \neq 0}} \frac{|b_2(\boldsymbol{v}_h, p_h - q_h)|}{\|\boldsymbol{v}_h\|_{\mathrm{H}(\mathrm{div};\Omega)}} = \frac{1}{\tilde{\beta}_2} \sup_{\substack{\boldsymbol{v}_h \in \mathrm{H}_h \\ \boldsymbol{v}_h \neq 0}} \frac{|a(\boldsymbol{u} - \boldsymbol{u}_h, \boldsymbol{v}_h) + b_1(\boldsymbol{v}_h, \omega - \omega_h) + b_2(\boldsymbol{v}_h, p - q_h)|}{\|\boldsymbol{v}_h\|_{\mathrm{H}(\mathrm{div};\Omega)}}, \\ \leq & C(\|\boldsymbol{u} - \boldsymbol{u}_h\|_{\mathrm{H}(\mathrm{div};\Omega)} + \|\omega - \omega_h\|_{1,\Omega} + \|p - q_h\|_{0,\Omega}). \end{aligned}$$

Therefore, estimate (3.15) is a direct consequence of (3.13), the previous estimate and the triangle inequality. □

The following theorem provides the rate of convergence of our mixed finite element scheme (3.4).

Theorem 3.2. *Let k be a non-negative integer and let $\mathrm{H}_h, \mathrm{Z}_h$ and Q_h be given by (3.1), (3.2), and (3.3). Let $(\boldsymbol{u}, \omega, p) \in \mathrm{H} \times \mathrm{Z} \times \mathrm{Q}$ and $(\boldsymbol{u}_h, \omega_h, p_h) \in \mathrm{H}_h \times \mathrm{Z}_h \times \mathrm{Q}_h$ be the unique solutions to the continuous and discrete problems (2.1) and (3.4), respectively. Assume that $\boldsymbol{u} \in \mathrm{H}^s(\Omega)^2$, $\operatorname{div} \boldsymbol{u} \in \mathrm{H}^s(\Omega)$, $\omega \in \mathrm{H}^{1+s}(\Omega)$ and $p \in \mathrm{H}^s(\Omega)$, for some $s \in (0, k+1]$. Then, there exists $\hat{C} > 0$ independent of h such that*

$$\|\boldsymbol{u} - \boldsymbol{u}_h\|_{\mathrm{H}(\mathrm{div};\Omega)} + \|\omega - \omega_h\|_{1,\Omega} + \|p - p_h\|_{0,\Omega} \leq \hat{C} h^s (\|\boldsymbol{u}\|_{\mathrm{H}^s(\mathrm{div};\Omega)} + \|\omega\|_{1+s,\Omega} + \|p\|_{s,\Omega}).$$

Proof. The proof follows from (3.13), (3.15), and standard error estimates for the operators $\mathcal{R}$, Π and $\mathcal{P}$ (see (3.9), (3.10) and (3.11), respectively). □

Remark 3.1. *As stated in the introduction, the present analysis can be easily adapted to introduce other families of mixed finite elements to solve problem (2.1). To this end, given an integer $k \geq 0$, we recall definitions of finite element subspaces based on piecewise continuous polynomials of degree $k+2$ for the vorticity, Brezzi–Douglas–Marini finite elements of order $k+1$ for the velocity, and piecewise polynomials of degree k for the pressure.*

We introduce the following finite element subspaces:

$$\mathcal{H}_h := \{\boldsymbol{v}_h \in \mathrm{H} : \boldsymbol{v}_h|_T \in \mathbb{P}_{k+1}(T)^2,\ \forall T \in \mathcal{T}_h\}, \tag{3.16}$$

$$\mathcal{Z}_h := \{\theta_h \in \mathrm{Z} : \theta_h|_T \in \mathbb{P}_{k+2}(T),\ \forall T \in \mathcal{T}_h\}, \tag{3.17}$$

$$\mathcal{Q}_h := \{q_h \in \mathrm{Q} : q_h|_T \in \mathbb{P}_k(T),\ \forall T \in \mathcal{T}_h\}. \tag{3.18}$$

Associated to these spaces we state the following Galerkin scheme, counterpart of the continuous variational formulation (2.1): *Find $(\boldsymbol{u}_h, \omega_h, p_h) \in \mathcal{H}_h \times \mathcal{Z}_h \times \mathcal{Q}_h$ such that*

$$\begin{aligned} a(\boldsymbol{u}_h, \boldsymbol{v}_h) + b_1(\boldsymbol{v}_h, \omega_h) + b_2(\boldsymbol{v}_h, p_h) &= G(\boldsymbol{v}_h) && \forall \boldsymbol{v}_h \in \mathcal{H}_h, \\ b_1(\boldsymbol{u}_h, \theta_h) - d(\omega_h, \theta_h) &= F(\theta_h) && \forall \theta_h \in \mathcal{Z}_h, \\ b_2(\boldsymbol{u}_h, q_h) &= 0 && \forall q_h \in \mathcal{Q}_h. \end{aligned} \tag{3.19}$$

We further recall the Brezzi–Douglas–Marini interpolation operator $\tilde{\mathcal{R}} : \mathrm{H}^s(\Omega)^2 \cap \mathrm{H} \to \mathcal{H}_h$ for all $s > 0$ (see [13]). An error estimate, similar to (3.9), is valid for the operator $\tilde{\mathcal{R}}$.

Using the arguments considered in this section, it is straightforward to prove the following result regarding existence and uniqueness of solution, and convergence of the discrete scheme (3.19).

Theorem 3.3. *Let k be a non-negative integer and let $\mathcal{H}_h \times \mathcal{Z}_h$ and $\mathcal{Q}_h$ be given by (3.16), (3.17), and (3.18). Then there exists a unique $(\boldsymbol{u}_h, \omega_h, p_h) \in \mathcal{H}_h \times \mathcal{Z}_h \times \mathcal{Q}_h$ solution of the Galerkin scheme (3.19). Assume further that the exact solution $(\boldsymbol{u}, \omega, p)$ satisfies $\boldsymbol{u} \in \mathrm{H}^s(\Omega)^2$, $\operatorname{div} \boldsymbol{u} \in \mathrm{H}^s(\Omega)$, $\omega \in \mathrm{H}^{1+s}(\Omega)$ and $p \in \mathrm{H}^s(\Omega)$, for some $s \in (0, k+1]$. Then, there exists $\hat{C} > 0$ independent of h such that*

$$\|\boldsymbol{u} - \boldsymbol{u}_h\|_{\mathrm{H}(\mathrm{div};\Omega)} + \|\omega - \omega_h\|_{1,\Omega} + \|p - p_h\|_{0,\Omega} \le \hat{C} h^s (\|\boldsymbol{u}\|_{\mathrm{H}^s(\mathrm{div};\Omega)} + \|\omega\|_{1+s,\Omega} + \|p\|_{s,\Omega}),$$

where $(\boldsymbol{u}, \omega, p) \in \mathrm{H} \times \mathrm{Z} \times \mathrm{Q}$ is the unique solution to variational problem (2.1).

4. A posteriori error analysis

In this section, we propose a residual-based a posteriori error estimator and we prove its reliability and efficiency. For sake of clarity we restrict our analysis to only one kind of boundary conditions, those defined in $\Gamma = \partial\Omega$. Therefore, the spaces to be consider in the sequel are the following:

$$\mathrm{H} := \{\boldsymbol{v} \in \mathrm{H}(\mathrm{div};\Omega) : \boldsymbol{v} \cdot \boldsymbol{n} = 0 \text{ on } \partial\Omega\}, \quad \mathrm{Z} := \mathrm{H}_0^1(\Omega), \quad \text{and} \quad \mathrm{Q} := \mathrm{L}_0^2(\Omega).$$

For each $T \in \mathcal{T}_h$ we let $\mathcal{E}(T)$ the set of edges of T, and we denote by $\mathcal{E}_h$ the set of all edges of $\mathcal{T}_h$, that is

$$\mathcal{E}_h = \mathcal{E}_h(\Omega) \cup \mathcal{E}_h(\Gamma),$$

where $\mathcal{E}_h(\Omega) := \{e \in \mathcal{E}_h : e \subset \Omega\}$, and $\mathcal{E}_h(\Gamma) := \{e \in \mathcal{E}_h : e \subset \Gamma\}$. In what follows, h_e stands for the diameter of a given edge $e \in \mathcal{E}_h$, $\boldsymbol{t}_e = (-n_2, n_1)$, where $\boldsymbol{n}_e = (n_1, n_2)$ is a fix unit normal vector of e. Now, let $q \in \mathrm{L}^2(\Omega)$ such that $q|_T \in C(T)$ for each $T \in \mathcal{T}_h$, then, given $e \in \mathcal{E}_h(\Omega)$, we denote by $[q]$ the jump of q across e, that is $[q] := (q|_{T'})|_e - (q|_{T''})|_e$, where T' and T'' are the triangles of $\mathcal{T}_h$ sharing the edge e. Moreover, let $\boldsymbol{v} \in \mathrm{L}^2(\Omega)^2$ such that $\boldsymbol{v}|_T \in C(T)^2$ for each $T \in \mathcal{T}_h$. Then, given $e \in \mathcal{E}_h(\Omega)$, we denote by $[\boldsymbol{v} \cdot \boldsymbol{t}]$ the tangential jump of $\boldsymbol{v}$ across e, that is, $[\boldsymbol{v} \cdot \boldsymbol{t}] := ((\boldsymbol{v}|_{T'})|_e - (\boldsymbol{v}|_{T''})|_e) \cdot \boldsymbol{t}_e$, where T' and T'' are the triangles of $\mathcal{T}_h$ sharing the edge e.

Next, let k be a non-negative integer and let $\mathrm{H}_h, \mathrm{Z}_h$ and Q_h be given by (3.1), (3.2), and (3.3). Let $(\boldsymbol{u}, \omega, p) \in \mathrm{H} \times \mathrm{Z} \times \mathrm{Q}$ and $(\boldsymbol{u}_h, \omega_h, p_h) \in \mathrm{H}_h \times \mathrm{Z}_h \times \mathrm{Q}_h$ be the unique solutions to the continuous and discrete problems (2.1) and (3.4) with data satisfying $\boldsymbol{f} \in \mathrm{L}^2(\Omega)^2$ and $\operatorname{rot} \boldsymbol{f} \in \mathrm{L}^2(T)$ for each $T \in \mathcal{T}_h$. We define for each $T \in \mathcal{T}_h$ the a posteriori error indicator

$$\begin{aligned}\boldsymbol{\theta}_T^2 :=& h_T^2 \|\operatorname{rot}(\boldsymbol{f} - \sigma \boldsymbol{u}_h - \nu\, \mathbf{curl}\, \omega_h)\|_{0,T}^2 + h_T^2 \|\boldsymbol{f} - \sigma \boldsymbol{u}_h - \nu\, \mathbf{curl}\, \omega_h - \nabla p_h\|_{0,T}^2 + h_T^2 \|\operatorname{rot} \boldsymbol{u}_h - \omega_h\|_{0,T}^2 \\ &+ \sum_{e \in \mathcal{E}(T) \cap \mathcal{E}_h(\Omega)} h_e \|[\boldsymbol{u}_h \cdot \boldsymbol{t}]\|_{0,e}^2 + \sum_{e \in \mathcal{E}(T) \cap \mathcal{E}_h(\Omega)} h_e \|[(\boldsymbol{f} - \sigma \boldsymbol{u}_h - \nu\, \mathbf{curl}\, \omega_h) \cdot \boldsymbol{t}]\|_{0,e}^2,\end{aligned}$$

and we introduce the global a posteriori error estimator:

$$\boldsymbol{\theta} := \left\{ \sum_{T \in \mathcal{T}_h} \boldsymbol{\theta}_T^2 \right\}^{1/2}. \tag{4.1}$$

4.1. Reliability of the a posteriori error estimator.

The main result of this section is stated as follows.

Theorem 4.1. *There exists $C_{rel} > 0$, independent of h, such that*

$$\|\boldsymbol{u} - \boldsymbol{u}_h\|_{\mathrm{H}(\mathrm{div};\Omega)} + \|\omega - \omega_h\|_{1,\Omega} + \|p - p_h\|_{0,\Omega} \le C_{rel} \boldsymbol{\theta}. \tag{4.2}$$

We begin the derivation of (4.2) by recalling that the continuous dependence result given by (2.5) is equivalent to the global inf-sup condition for the continuous reduced formulation (2.4). Then, applying this estimate to the total error $(\boldsymbol{u} - \boldsymbol{u}_h, \omega - \omega_h) \in \mathrm{X} \times \mathrm{Z}$, we obtain

$$\|\boldsymbol{u} - \boldsymbol{u}_h\|_{\mathrm{H}(\mathrm{div};\Omega)} + \|\omega - \omega_h\|_{1,\Omega} \le C \sup_{\substack{(\boldsymbol{v},\theta) \in \mathrm{X} \times \mathrm{Z} \\ (\boldsymbol{v},\theta) \neq 0}} \frac{|R(\boldsymbol{v}, \theta)|}{\|(\boldsymbol{v}, \theta)\|}, \tag{4.3}$$

where $R : \mathrm{X} \times \mathrm{Z} \to \mathbb{R}$ is the residual operator defined by

$$R(\boldsymbol{v}, \theta) := a(\boldsymbol{u} - \boldsymbol{u}_h, \boldsymbol{v}) + b_1(\boldsymbol{v}, \omega - \omega_h) + b_1(\boldsymbol{u} - \boldsymbol{u}_h, \theta) - d(\omega - \omega_h, \theta)$$

for all $(\boldsymbol{v}, \theta) \in \mathrm{X} \times \mathrm{Z}$. Moreover, we have that

$$R(\boldsymbol{v}, \theta) := R_1(\boldsymbol{v}) + R_2(\theta),$$

where

$$R_1(\boldsymbol{v}) := \int_\Omega \boldsymbol{f} \cdot \boldsymbol{v} - \sigma \int_\Omega \boldsymbol{u}_h \cdot \boldsymbol{v} - \nu \int_\Omega \mathbf{curl}\, \omega_h \cdot \boldsymbol{v}, \quad R_2(\theta) := -\nu \int_\Omega \mathbf{curl}\, \theta \cdot \boldsymbol{u}_h + \nu \int_\Omega \omega_h \theta.$$

Hence, the supremum in (4.3) can be bounded in terms of $R_i, i \in \{1, 2\}$, which yields

$$\|\boldsymbol{u} - \boldsymbol{u}_h\|_{\mathrm{H}(\mathrm{div};\Omega)} + \|\omega - \omega_h\|_{1,\Omega} \leq C \left(\sup_{\substack{\boldsymbol{v} \in \mathrm{X} \\ \boldsymbol{v} \neq 0}} \frac{|R_1(\boldsymbol{v})|}{\|\boldsymbol{v}\|_{\mathrm{H}(\mathrm{div};\Omega)}} + \sup_{\substack{\theta \in \mathrm{Z} \\ \theta \neq 0}} \frac{|R_2(\theta)|}{\|\theta\|_{1,\Omega}} \right). \tag{4.4}$$

In what follows, we provide suitable upper bounds for each term on the right hand side of (4.4). Before doing this, we first need to introduce some previous results.

In the sequel, we will utilize the Clément interpolation operator $I_h : \mathrm{H}^1(\Omega) \to Y_h$, where

$$Y_h := \{\theta_h \in \mathrm{H}^1(\Omega) : \theta_h|_T \in \mathbb{P}_1(T),\ \forall T \in \mathcal{T}_h\}.$$

The following lemma establishes the local approximation properties of I_h. See [18] for details.

Lemma 4.1. *There exist positive constants $\tilde{c}$ and $\hat{c}$ such that for all $\theta \in \mathrm{H}^1(\Omega)$ there hold*

$$\|\theta - I_h\theta\|_{0,T} \leq \tilde{c} h_T \|\theta\|_{1,\Delta(T)} \quad \forall T \in \mathcal{T}_h,$$
$$\|\theta - I_h\theta\|_{0,e} \leq \hat{c} h_e^{1/2} \|\theta\|_{1,\Delta(e)} \quad \forall e \in \mathcal{E}_h,$$

where $\Delta(T) := \cup\{T' \in \mathcal{T}_h : T' \cap T \neq 0\}$ and $\Delta(e) := \cup\{T' \in \mathcal{T}_h : T' \cap e \neq 0\}$.

The following lemma establishes the corresponding upper bound for R_1.

Lemma 4.2. *There exists $C_1 > 0$, independent of h, such that*

$$\sup_{\substack{\boldsymbol{v} \in \mathrm{X} \\ \boldsymbol{v} \neq 0}} \frac{|R_1(\boldsymbol{v})|}{\|\boldsymbol{v}\|_{\mathrm{H}(\mathrm{div};\Omega)}} \leq C_1 \Bigg\{ \sum_{T \in \mathcal{T}_h} h_T \|\operatorname{rot}(\boldsymbol{f} - \sigma \boldsymbol{u}_h - \nu\, \mathbf{curl}\, \omega_h)\|_{0,T} + \sum_{e \in \mathcal{E}_h(\Omega)} h_e^{1/2} \|[(\boldsymbol{f} - \sigma \boldsymbol{u}_h - \nu\, \mathbf{curl}\, \omega_h) \cdot \boldsymbol{t}]\|_{0,e} \Bigg\}^{1/2}.$$

Proof. Given $\boldsymbol{v} \in \mathrm{X}$ we know that $\operatorname{div} \boldsymbol{v} = 0$ in Ω and $\boldsymbol{v} \cdot \boldsymbol{n} = 0$ on Γ. Then, applying [30, Theorem 3.1], we can assert that there exists a unique $\phi \in \mathrm{H}_0^1(\Omega)$, such that $\boldsymbol{v} = \mathbf{curl}\, \phi$ in Ω, and

$$\|\phi\|_{1,\Omega} \leq C \|\boldsymbol{v}\|_{\mathrm{H}(\mathrm{div};\Omega)}.$$

Hence, since $R_1(\boldsymbol{v}_h) = 0 \quad \forall \boldsymbol{v}_h \in \mathrm{X}_h$, which follows from the first equation of the Galerkin scheme (3.7), we obtain

$$R_1(\boldsymbol{v}) = R_1(\mathbf{curl}(\phi)) = R_1(\mathbf{curl}(\phi - I_h\phi)) = \int_\Omega (\boldsymbol{f} - \sigma \boldsymbol{u}_h - \nu\, \mathbf{curl}\, \omega_h) \cdot \mathbf{curl}(\phi - I_h\phi),$$

and integrating by parts we easily get

$$R_1(\mathbf{curl}(\phi - I_h\phi)) = \sum_{T \in \mathcal{T}_h} \Bigg[\int_T \operatorname{rot}(\boldsymbol{f} - \sigma \boldsymbol{u}_h - \nu\, \mathbf{curl}\, \omega_h)(\phi - I_h\phi) - \int_{\partial T} (\phi - I_h\phi)(\boldsymbol{f} - \sigma \boldsymbol{u}_h - \nu\, \mathbf{curl}\, \omega_h) \cdot \boldsymbol{t} \Bigg]$$

$$= \sum_{T\in\mathcal{T}_h}\int_T \operatorname{rot}(\boldsymbol{f}-\sigma\boldsymbol{u}_h-\nu\,\mathbf{curl}\,\omega_h)(\phi-I_h\phi)$$
$$-\sum_{e\in\mathcal{E}_h(\Omega)}\int_e(\phi-I_h\phi)[(\boldsymbol{f}-\sigma\boldsymbol{u}_h-\nu\,\mathbf{curl}\,\omega_h)\cdot\boldsymbol{t}].$$

Therefore, the proof follows from the Cauchy-Schwarz inequality, the approximation properties of the operator I_h (see Lemma 4.1), and the fact that the number of triangles in $\Delta(T)$ and $\Delta(e)$ is bounded.

□

Now we establish the upper bound for R_2.

Lemma 4.3. *There exists $C_2>0$, independent of h, such that*

$$\sup_{\substack{\theta\in \mathrm{Z}\\ \theta\neq 0}}\frac{|R_2(\theta)|}{\|\theta\|_{1,\Omega}}\le C_2\left\{\sum_{T\in\mathcal{T}_h}h_T\|\operatorname{rot}\boldsymbol{u}_h-\omega_h\|_{0,T}+\sum_{e\in\mathcal{E}_h(\Omega)}h_e^{1/2}\|[\boldsymbol{u}_h\cdot\boldsymbol{t}]\|_{0,e}\right\}^{1/2}.$$

Proof. We first observe that $R_2(\theta_h)=0\quad\forall\theta_h\in\mathrm{Z}_h$, which follows from the second equation in the Galerkin scheme (3.7). Then, for all $\theta\in\mathrm{H}_0^1(\Omega)$ it follows that

$$R_2(\theta)=R_2(\theta-I_h\theta)=\nu\int_\Omega\omega_h(\theta-I_h\theta)-\nu\int_\Omega\mathbf{curl}(\theta-I_h\theta)\cdot\boldsymbol{u}_h,$$

and integrating by parts, we obtain

$$R_2(\theta-I_h\theta)=\nu\sum_{T\in\mathcal{T}_h}\int_T\omega_h(\theta-I_h\theta)-\nu\sum_{T\in\mathcal{T}_h}\left(\int_T(\theta-I_h\theta)\operatorname{rot}\boldsymbol{u}_h-\int_{\partial T}(\theta-I_h\theta)(\boldsymbol{u}_h\cdot\boldsymbol{t})\right),$$
$$=\nu\sum_{T\in\mathcal{T}_h}\int_T(\omega_h-\operatorname{rot}\boldsymbol{u}_h)(\theta-I_h\theta)+\nu\sum_{e\in\mathcal{E}_h(\Omega)}\int_e(\theta-I_h\theta)[\boldsymbol{u}_h\cdot\boldsymbol{t}].$$

Then, the proof readily follows by the Cauchy-Schwarz inequality, the approximation properties of the operator I_h (see Lemma 4.1), and the fact that the number of triangles in $\Delta(T)$ and $\Delta(e)$ is bounded. □

To conclude the derivation of (4.2) we need to estimate the error $\|p-p_h\|_{0,\Omega}$. To this end we will need the following result.

Lemma 4.4. *Let $(\boldsymbol{u},\omega,p)\in\mathrm{H}\times\mathrm{Z}\times\mathrm{Q}$ and $(\boldsymbol{u}_h,\omega_h,p_h)\in\mathrm{H}_h\times\mathrm{Z}_h\times\mathrm{Q}_h$ be the unique solutions of (2.1) and (3.4), respectively. Then for all $\boldsymbol{v}\in\mathrm{H}$ and for all $\boldsymbol{v}_h\in\mathrm{H}_h$, there holds*

$$b_2(\boldsymbol{v},p-p_h)=-a(\boldsymbol{u}-\boldsymbol{u}_h,\boldsymbol{v})-b_1(\boldsymbol{v},\omega-\omega_h)+L(\boldsymbol{v}-\boldsymbol{v}_h),\tag{4.5}$$

with

$$L(\boldsymbol{v}-\boldsymbol{v}_h)=\int_\Omega\boldsymbol{f}\cdot(\boldsymbol{v}-\boldsymbol{v}_h)-a(\boldsymbol{u}_h,\boldsymbol{v}-\boldsymbol{v}_h)-b_1(\boldsymbol{v}-\boldsymbol{v}_h,\omega_h)-b_2(\boldsymbol{v}-\boldsymbol{v}_h,p_h).$$

Proof. Let $\boldsymbol{v}\in\mathrm{H}$ and $\boldsymbol{v}_h\in\mathrm{H}_h$. From the first equations of (2.1) and (3.4), respectively, we deduce that

$$b_2(\boldsymbol{v},p-p_h)=\int_\Omega\boldsymbol{f}\cdot\boldsymbol{v}-a(\boldsymbol{u},\boldsymbol{v})-b_1(\boldsymbol{v},\omega)-b_2(\boldsymbol{v},p_h),\tag{4.6}$$

and

$$b_2(\boldsymbol{v}_h,p_h)=\int_\Omega\boldsymbol{f}\cdot\boldsymbol{v}_h-a(\boldsymbol{u}_h,\boldsymbol{v}_h)-b_1(\boldsymbol{v}_h,\omega_h).\tag{4.7}$$

Then, adding and subtracting $a(\boldsymbol{u}_h,\boldsymbol{v})$, $b_1(\boldsymbol{v},\omega_h)$ and $b_2(\boldsymbol{v}_h,p_h)$ in the right hand side of (4.6), we obtain

$$b_2(\boldsymbol{v},p-p_h)=\int_\Omega\boldsymbol{f}\cdot\boldsymbol{v}-a(\boldsymbol{u}-\boldsymbol{u}_h,\boldsymbol{v})-b_1(\boldsymbol{v},\omega-\omega_h)-a(\boldsymbol{u}_h,\boldsymbol{v})$$
$$-b_1(\boldsymbol{v},\omega_h)-b_2(\boldsymbol{v}-\boldsymbol{v}_h,p_h)-b_2(\boldsymbol{v}_h,p_h).$$

Therefore, it suffices to replace $b_2(\boldsymbol{v}_h, p_h)$ by (4.7) in the last identity to conclude. □

We now recall the local approximation properties of the Raviart-Thomas interpolator $\mathcal{R} : \mathrm{H}^1(\Omega)^2 \to \mathrm{H}_h$ (see [13]): there exist constants c_1, $c_2 > 0$, independent of h, such that for all $\boldsymbol{v} \in \mathrm{H}^1(\Omega)^2$, there hold

$$\|\boldsymbol{v} - \mathcal{R}\boldsymbol{v}\|_{0,T} \le c_1\, h_T\, \|\boldsymbol{v}\|_{1,T} \qquad \forall\, T \in \mathcal{T}_h\,,$$

and

$$\|\boldsymbol{v}\cdot\boldsymbol{n} - \mathcal{R}\boldsymbol{v}\cdot\boldsymbol{n}\|_{0,e} \le c_2\, h_e^{1/2}\, \|\boldsymbol{v}\|_{1,T_e} \qquad \forall \text{ edge } e \text{ of } \mathcal{T}_h\,,$$

where T_e is a triangle of $\mathcal{T}$ containing e on its boundary.

We are now in position of establishing the upper bound for $\|p - p_h\|_{0,\Omega}$.

Lemma 4.5. *There exists $C_3 > 0$, independent of h, such that*

$$\|p - p_h\|_{0,\Omega} \le C_3 \left(\|\boldsymbol{u} - \boldsymbol{u}_h\|_{\mathrm{H}(\mathrm{div};\Omega)} + \|\omega - \omega_h\|_{1,\Omega} + \left\{ \sum_{T\in\mathcal{T}_h} h_T^2 \|\boldsymbol{f} - \sigma\boldsymbol{u}_h - \nu\,\mathbf{curl}\,\omega_h - \nabla p_h\|_{0,T}^2 \right\}^{1/2} \right).$$

Proof. First, let us notice that from the inf-sup condition (2.2), we have

$$\|p - p_h\|_{0,\Omega} \le \frac{1}{\beta_2} \sup_{\substack{\boldsymbol{v}\in\mathrm{H}\\ \boldsymbol{v}\neq 0}} \frac{|b_2(\boldsymbol{v}, p - p_h)|}{\|\boldsymbol{v}\|_{\mathrm{H}(\mathrm{div};\Omega)}}. \tag{4.8}$$

Then, it remains to bound the right hand side of (4.8) to conclude.

Let $\boldsymbol{v} \in \mathrm{H}$. Since $\boldsymbol{v}\cdot\boldsymbol{n} = 0$ on Γ, it follows that $\mathrm{div}\,\boldsymbol{v} \in L_0^2(\Omega)$, and then, applying [30, Corollary 2.4], we conclude that there exists a unique $\boldsymbol{z} \in \mathrm{H}_0^1(\Omega)^2$, such that

$$\mathrm{div}\,\boldsymbol{z} = \mathrm{div}\,\boldsymbol{v} \quad \text{in} \quad \Omega, \quad \text{and} \quad \|\boldsymbol{z}\|_{1,\Omega} \le C\|\boldsymbol{v}\|_{\mathrm{H}(\mathrm{div};\Omega)}. \tag{4.9}$$

Hence, we define $\boldsymbol{z}_h = \mathcal{R}(\boldsymbol{z}) \in \mathrm{H}_h$, and apply identity (4.5) to obtain

$$b_2(\boldsymbol{v}, p - p_h) = b_2(\boldsymbol{z}, p - p_h) = -a(\boldsymbol{u} - \boldsymbol{u}_h, \boldsymbol{z}) - b_1(\boldsymbol{z}, \omega - \omega_h) + L(\boldsymbol{z} - \boldsymbol{z}_h). \tag{4.10}$$

Now, recalling the definition of L, a, b_1 and b_2, we integrate by part on each triangle, to obtain

$$\begin{aligned} L(\boldsymbol{z} - \boldsymbol{z}_h) = &\int_\Omega \boldsymbol{f}\cdot(\boldsymbol{z} - \boldsymbol{z}_h) - \sigma\int_\Omega \boldsymbol{u}_h\cdot(\boldsymbol{z} - \boldsymbol{z}_h) - \nu\int_\Omega \mathbf{curl}\,\omega_h\cdot(\boldsymbol{z} - \boldsymbol{z}_h) + \int_\Omega p_h\,\mathrm{div}(\boldsymbol{z} - \boldsymbol{z}_h),\\ = &\sum_{T\in\mathcal{T}_h}\int_T (\boldsymbol{f} - \sigma\boldsymbol{u}_h - \nu\,\mathbf{curl}\,\omega_h - \nabla p_h)\cdot(\boldsymbol{z} - \boldsymbol{z}_h). \end{aligned} \tag{4.11}$$

In this way, from (4.10), (4.11), the definition of a, b_1, the local approximation properties of the interpolation operator $\mathcal{R}$, and the Cauchy-Schwarz inequality, we get

$$\begin{aligned} |b_2(\boldsymbol{v}, p - p_h)| \le\ & \sigma\|\boldsymbol{u} - \boldsymbol{u}_h\|_{\mathrm{H}(\mathrm{div};\Omega)}\|\boldsymbol{z}\|_{1,\Omega} + \nu\|\omega - \omega_h\|_{1,\Omega}\|\boldsymbol{z}\|_{1,\Omega}\\ &+ \sum_{T\in\mathcal{T}_h} \|\boldsymbol{f} - \sigma\boldsymbol{u}_h - \mathbf{curl}\,\omega_h - \nabla p_h\|_{0,T}\|\boldsymbol{z} - \boldsymbol{z}_h\|_{0,T}\\ \le\ & \left(\sigma\|\boldsymbol{u} - \boldsymbol{u}_h\|_{\mathrm{H}(\mathrm{div};\Omega)} + \nu\|\omega - \omega_h\|_{1,\Omega}\right)\|\boldsymbol{z}\|_{1,\Omega}\\ &+ C\left\{\sum_{T\in\mathcal{T}_h} h_T^2\|\boldsymbol{f} - \sigma\boldsymbol{u}_h - \nu\,\mathbf{curl}\,\omega_h - \nabla p_h\|_{0,T}^2\right\}^{1/2}\|\boldsymbol{z}\|_{1,\Omega}. \end{aligned} \tag{4.12}$$

Therefore, the result follows from (4.8), (4.12) and the upper bound of $\boldsymbol{z}$ in (4.9). □

We end this section by observing that the reliability estimate (4.2) (cf. Theorem 4.1) is a direct consequence of Lemmas 4.2, 4.3 and 4.5.

4.2. **Efficiency of the a posteriori error estimator.** The main result of this section is stated next.

Theorem 4.2. *There exists $C_{eff} > 0$, independent of h, such that*

$$C_{eff}\boldsymbol{\theta} \leq \|\boldsymbol{u} - \boldsymbol{u}_h\|_{\mathrm{H(div;\Omega)}} + \|\omega - \omega_h\|_{1,\Omega} + \|p - p_h\|_{0,\Omega} + h.o.t.,$$

where h.o.t. stands, eventually, for one or several terms of higher order.

In order to proof the efficiency of the a posteriori error estimator, in what follows we bound each term defining $\boldsymbol{\theta}_T$ (cf. (4.1)) in terms of local errors. To do this, we proceed similarly to [28] (see also [8]), using known results, mainly from [15], and applying inverse inequalities and the localization technique based on element-bubble and edge-bubble functions. To this end, we now introduce some notations and further preliminary results.

Given $\mathcal{T}_h$, $T \in \mathcal{T}_h$, and $e \in \mathcal{E}(T)$, we introduce ψ_T and ψ_e be the usual triangle-bubble and edge-bubble functions, respectively (see (1.5) and (1.6) in [38]). In particular, ψ_T satisfies $\psi_T \in \mathbb{P}_3(T)$, $supp(\psi_T) \subseteq T$, $\psi_T = 0$ on ∂T, and $0 \leq \psi_T \leq 1$ in T. Similarly, $\psi_e|_T \in \mathbb{P}_2(T)$, $supp(\psi_e) \subseteq \omega_e := \cup\{T' \in \mathcal{T}_h : e \in \mathcal{E}(T')\}$, $\psi_e = 0$ on $\partial T \setminus e$, and $0 \leq \psi_e \leq 1$ in ω_e. We recall (also from [38]) that, given $k \in \mathbb{N} \cup \{0\}$, there exists an extension operator $L : C(e) \to C(T)$ that satisfies $L(q) \in \mathbb{P}_k(T)$ and $L(q)|_e = q \quad \forall q \in \mathbb{P}_k(e)$. A corresponding vectorial version of L, that is the component-wise application of L, will be also considered.

Additional properties of ψ_T, ψ_e and L are collected in the following lemma (see [38]).

Lemma 4.6. *Given $k \in \mathbb{N} \cup \{0\}$, there exist positive constants c_1, c_2 and c_3, depending only on k and the shape regularity of the triangulations (minimum angle condition), such that for each triangle T and $e \in \mathcal{E}(T)$, there hold*

$$\|q\|_{0,T}^2 \leq c_1 \|\psi_T^{1/2} q\|_{0,T}^2 \quad \forall q \in \mathbb{P}_k(T)$$
$$\|q\|_{0,e}^2 \leq c_2 \|\psi_e^{1/2} q\|_{0,e}^2 \quad \forall q \in \mathbb{P}_k(e).$$

and

$$\|\psi_e^{1/2} L(q)\|_{0,T}^2 \leq c_3 h_e \|q\|_{0,e}^2 \quad \forall q \in \mathbb{P}_k(e).$$

The following classical result which states an inverse estimate will also be used.

Lemma 4.7. *Let $k, l, m \in \mathbb{N} \cup \{0\}$ such that $l \leq m$. Then, there exists $c_4 > 0$, depending only on k, l, m and the shape regularity of the triangulations, such that for each triangle T there holds*

$$|q|_{m,T} \leq c_4 h_T^{l-m} |q|_{l,T} \quad \forall q \in \mathbb{P}_k(T).$$

The following lemmas provide the corresponding upper bounds for each term defining $\boldsymbol{\theta}_T$.

Lemma 4.8. *There exists $C > 0$, independent of h, such that for each $T \in \mathcal{T}_h$ there holds*

$$h_T^2 \|\operatorname{rot} \boldsymbol{u}_h - \omega_h\|_{0,T}^2 \leq C(\|\boldsymbol{u} - \boldsymbol{u}_h\|_{0,T}^2 + h_T^2 \|\omega - \omega_h\|_{0,T}^2).$$

Proof. First, from Lemma 4.6 and then, using that $\operatorname{rot} \boldsymbol{u} - \omega = 0$ in Ω (see Theorem 2.2), integration by parts and the Cauchy-Schwarz inequality, we get

$$\begin{aligned}
\|\operatorname{rot} \boldsymbol{u}_h - \omega_h\|_{0,T}^2 \leq & \|\psi_T^{1/2}(\operatorname{rot} \boldsymbol{u}_h - \omega_h)\|_{0,T}^2 \\
= & \left(\int_T \psi_T (\operatorname{rot} \boldsymbol{u}_h - \omega_h) \operatorname{rot}(\boldsymbol{u}_h - \boldsymbol{u}) + \int_T \psi_T (\operatorname{rot} \boldsymbol{u}_h - \omega_h)(\omega - \omega_h) \right) \\
= & \left(\int_T \mathbf{curl}(\psi_T (\operatorname{rot} \boldsymbol{u}_h - \omega_h)) \cdot (\boldsymbol{u}_h - \boldsymbol{u}) + \int_T \psi_T (\operatorname{rot} \boldsymbol{u}_h - \omega_h)(\omega - \omega_h) \right) \\
\leq & \|\mathbf{curl}(\psi_T (\operatorname{rot} \boldsymbol{u}_h - \omega_h))\|_{0,T} \|\boldsymbol{u} - \boldsymbol{u}_h\|_{0,T} + \|\psi_T (\operatorname{rot} \boldsymbol{u}_h - \omega_h)\|_{0,T} \|\omega - \omega_h\|_{0,T}.
\end{aligned}$$

Since $\psi_T(\operatorname{rot} \boldsymbol{u}_h - \omega_h)$ is a polynomial on each $T \in \mathcal{T}_h$, from Lemma 4.7 we have

$$|\psi_T (\operatorname{rot} \boldsymbol{u}_h - \omega_h)|_{1,T} \leq c_4 h_T^{-1} \|\psi_T (\operatorname{rot} \boldsymbol{u}_h - \omega_h)\|_{0,T},$$

which completes the proof. □

Lemma 4.9. *There exists $C > 0$, independent of h, such that for each $T \in \mathcal{T}_h$ there holds*

$$h_e\|[\boldsymbol{u}_h \cdot \boldsymbol{t}]\|_{0,e}^2 \leq C \sum_{T\in\omega_e} (\|\boldsymbol{u} - \boldsymbol{u}_h\|_{0,T}^2 + \|\omega - \omega_h\|_{0,T}^2).$$

Proof. The estimate follows repeating the arguments used in the proof of [15, Lemma 6.2], and using Lemma 4.8. □

Lemma 4.10. *There exists $C > 0$, independent of h, such that for each $T \in \mathcal{T}_h$ there holds*

$$h_T^2\|\operatorname{rot}(\boldsymbol{f} - \sigma\boldsymbol{u}_h - \nu\,\mathbf{curl}\,\omega_h)\|_{0,T}^2 \leq C(\|u - u_h\|_{0,T}^2 + |\omega - \omega_h|_{1,T}^2 + h_T^2\|\operatorname{rot}\boldsymbol{f} - \mathcal{P}_T^l(\operatorname{rot}\boldsymbol{f})\|_{0,T}^2),$$

where $\mathcal{P}_T^l$ is the $L^2(T)^2$-orthogonal projection onto $\mathbb{P}_l(T)^2$ where $l \geq k$, with respect to the inner product $(\boldsymbol{f},\boldsymbol{g})_{0,T} := \int_T \psi_T \boldsymbol{f}\cdot\boldsymbol{g}$ for each $\boldsymbol{f},\boldsymbol{g} \in L^2(T)^2$.

Proof. First, adding and subtracting the term $\mathcal{P}_T^l(\operatorname{rot}\boldsymbol{f})$, and then using the triangle inequality we obtain

$$\begin{aligned}\|\operatorname{rot}(\boldsymbol{f} - \sigma\boldsymbol{u}_h - \nu\,\mathbf{curl}\,\omega_h)\|_{0,T}^2 \leq& 2\left(\|\operatorname{rot}\boldsymbol{f} - \mathcal{P}_T^l(\operatorname{rot}\boldsymbol{f})\|_{0,T}^2 + \|\mathcal{P}_T^l(\operatorname{rot}\boldsymbol{f}) - \operatorname{rot}(\sigma\boldsymbol{u}_h - \nu\,\mathbf{curl}\,\omega_h)\|_{0,T}^2\right)\\ =&2\left(\|\operatorname{rot}\boldsymbol{f} - \mathcal{P}_T^l(\operatorname{rot}\boldsymbol{f})\|_{0,T}^2 + \|\mathcal{P}_T^l(\operatorname{rot}(\boldsymbol{f} - \sigma\boldsymbol{u}_h - \nu\,\mathbf{curl}\,\omega_h))\|_{0,T}^2\right).\end{aligned}$$

Now, from Lemma 4.6, we get

$$\begin{aligned}\|\mathcal{P}_T^l(\operatorname{rot}(\boldsymbol{f} - \sigma\boldsymbol{u}_h - \nu\,\mathbf{curl}\,\omega_h))\|_{0,T}^2 \leq& \|\psi_T^{1/2}\mathcal{P}_T^l(\operatorname{rot}(\boldsymbol{f} - \sigma\boldsymbol{u}_h - \nu\,\mathbf{curl}\,\omega_h))\|_{0,T}^2\\ =& \int_T \psi_T\mathcal{P}_T^l(\operatorname{rot}(\boldsymbol{f} - \sigma\boldsymbol{u}_h - \nu\,\mathbf{curl}\,\omega_h))\mathcal{P}_T^l(\operatorname{rot}(\boldsymbol{f} - \sigma\boldsymbol{u}_h - \nu\,\mathbf{curl}\,\omega_h))\\ =& \int_T \psi_T\mathcal{P}_T^l(\operatorname{rot}(\boldsymbol{f} - \sigma\boldsymbol{u}_h - \nu\,\mathbf{curl}\,\omega_h))\operatorname{rot}(\boldsymbol{f} - \sigma\boldsymbol{u}_h - \nu\,\mathbf{curl}\,\omega_h),\end{aligned}$$

where we have used the fact that $\mathcal{P}_T^l$ is the $L^2(T)^2$-orthogonal projection onto $\mathbb{P}_l(T)^2$. Then, since $\operatorname{rot}(\boldsymbol{f} - \sigma\boldsymbol{u} - \nu\,\mathbf{curl}\,\omega) = 0$ in Ω (see Theorem 2.2), the proof follows by an integration by parts, the Cauchy-Schwarz inequality and Lemma 4.7. □

Lemma 4.11. *There exists $C > 0$, independent of h, such that for each $T \in \mathcal{T}_h$ there holds*

$$h_T^2\|\boldsymbol{f} - \sigma\boldsymbol{u}_h - \nu\,\mathbf{curl}\,\omega_h - \nabla p_h\|_{0,T}^2 \leq C\left(h_T^2\|u - u_h\|_{0,T}^2 + h_T^2|\omega - \omega_h|_{1,T}^2 + \|p - p_h\|_{0,T}^2 + h_T^2\|\boldsymbol{f} - \mathcal{P}_T^l(\boldsymbol{f})\|_{0,T}^2\right),$$

where $\mathcal{P}_T^l$ is the $L^2(T)^2$-orthogonal projection onto $\mathbb{P}_l(T)^2$ where $l \geq k$, with respect to the inner product $(\boldsymbol{f},\boldsymbol{g})_{0,T} := \int_T \psi_T \boldsymbol{f}\cdot\boldsymbol{g}$ for each $\boldsymbol{f},\boldsymbol{g} \in L^2(T)^2$.

Proof. The estimate follows after combining the arguments used in the proof of [15, Lemma 6.3] and the proof of Lemma 4.10. □

Lemma 4.12. *There exists $C > 0$, independent of h, such that for each $T \in \mathcal{T}_h$ there holds*

$$\begin{aligned}&h_e\|[(\boldsymbol{f} - \sigma\boldsymbol{u}_h - \nu\,\mathbf{curl}\,\omega_h)\cdot\boldsymbol{t}]\|_{0,e}^2 \leq\\ &\qquad C\sum_{T\in\omega_e}\left(\|u - u_h\|_{0,T}^2 + |\omega - \omega_h|_{1,T}^2 + \|\boldsymbol{f} - \tilde{\mathcal{P}}_T^l(\boldsymbol{f})\|_{0,T}^2 + h_T^2|\boldsymbol{f} - \tilde{\mathcal{P}}^l(\boldsymbol{f})|_{1,T}^2\right),\end{aligned}$$

where $\tilde{\mathcal{P}}_T^l$ is the $L^2(T)^2$-orthogonal projection onto $\mathbb{P}_l(T)^2$ with $l \geq k$.

Proof. Adding and subtracting $\tilde{\mathcal{P}}^l(\boldsymbol{f})$, followed by a use of triangle inequality yields.

$$\begin{aligned}&h_e^{1/2}\|[(\boldsymbol{f} - \sigma\boldsymbol{u}_h - \nu\,\mathbf{curl}\,\omega_h)\cdot\boldsymbol{t}]\|_{0,e} \leq\\ &\qquad h_e^{1/2}\|[(\boldsymbol{f} - \tilde{\mathcal{P}}^l(\boldsymbol{f}))\cdot\boldsymbol{t}]\|_{0,e} + h_e^{1/2}\|[\tilde{\mathcal{P}}^l(\boldsymbol{f} - \sigma\boldsymbol{u}_h - \nu\,\mathbf{curl}\,\omega_h)\cdot\boldsymbol{t}]\|_{0,e}.\end{aligned} \tag{4.13}$$

The first term in the right hand side can be bound using the local trace inequality as follows:

$$h_e^{1/2}\|[(\boldsymbol{f}-\tilde{\mathcal{P}}^l(\boldsymbol{f}))\cdot\boldsymbol{t}]\|_{0,e}\leq h_e^{1/2}\left(h_e^{-1/2}\sum_{T\in\omega_e}\|\boldsymbol{f}-\tilde{\mathcal{P}}^l(\boldsymbol{f})\|_{0,T}+h_e^{1/2}\sum_{T\in\omega_e}|\boldsymbol{f}-\tilde{\mathcal{P}}^l(\boldsymbol{f})|_{1,T}\right). \tag{4.14}$$

Now, we denote $\xi_h := \boldsymbol{f}-\sigma\boldsymbol{u}_h-\nu\,\mathbf{curl}\,\omega_h$. From Lemma 4.6, integration by parts, and the fact that $\nabla p=\boldsymbol{f}-\sigma\boldsymbol{u}-\nu\,\mathbf{curl}\,\omega:=\xi$ (see Theorem 2.2), we bound the second term in the right hand side of (4.13), as follows

$$\begin{aligned}\|[\tilde{\mathcal{P}}_T^l(\xi_h)\cdot\boldsymbol{t}]\|_{0,e}^2 \leq&\|\psi_e^{1/2}[\tilde{\mathcal{P}}_T^l(\xi_h)\cdot\boldsymbol{t}]\|_{0,e}^2=\int_e\psi_e L([\tilde{\mathcal{P}}_T^l(\xi_h)\cdot\boldsymbol{t}])[\tilde{\mathcal{P}}_T^l(\xi_h)\cdot\boldsymbol{t}]\\ &=\sum_{T\in\omega_e}\left(\int_T\tilde{\mathcal{P}}_T^l(\xi_h)\cdot\mathbf{curl}(\psi_e L([\tilde{\mathcal{P}}_T^l(\xi_h)\cdot\boldsymbol{t}]))+\int_T\psi_e L([\tilde{\mathcal{P}}_T^l(\xi_h)\cdot\boldsymbol{t}])\,\mathrm{rot}\,\tilde{\mathcal{P}}_T^l(\xi_h)\right)\\ &=\sum_{T\in\omega_e}\left(\int_T(\tilde{\mathcal{P}}_T^l(\xi_h)-\xi)\cdot\mathbf{curl}(\psi_e L([\tilde{\mathcal{P}}_T^l(\xi_h)\cdot\boldsymbol{t}]))+\int_T\psi_e L([\tilde{\mathcal{P}}_T^l(\xi_h)\cdot\boldsymbol{t}])\,\mathrm{rot}\,\tilde{\mathcal{P}}_T^l(\xi_h)\right),\end{aligned}$$

where we have also used that $\nabla p\in\mathrm{H}(\mathrm{rot};\Omega)$. Therefore, a direct application of Cauchy-Schwarz inequality and Lemma 4.7 implies that

$$\|[\tilde{\mathcal{P}}_T^l(\xi_h)\cdot\boldsymbol{t}]\|_{0,e}^2\leq\sum_{T\in\omega_e}\left(h_T^{-1}\|\tilde{\mathcal{P}}_T^l(\xi_h)-\xi)\|_{0,T}+\|\,\mathrm{rot}\,\tilde{\mathcal{P}}_T^l(\xi_h)\|_{0,T}\right)\|\psi_e L([\tilde{\mathcal{P}}_T^l(\xi_h)\cdot\boldsymbol{t}])\|_{0,T}.$$

Using that $0\leq\psi_e\leq 1$ and applying the third estimate of Lemma 4.6, we get

$$\|\psi_e L([\tilde{\mathcal{P}}_T^l(\xi_h)\cdot\boldsymbol{t}])\|_{0,T}\leq\|\psi_e^{1/2}L([\tilde{\mathcal{P}}_T^l(\xi_h)\cdot\boldsymbol{t}])\|_{0,T}\leq Ch_e^{1/2}\|[\tilde{\mathcal{P}}_T^l(\xi_h)\cdot\boldsymbol{t}]\|_{0,T},$$

and hence, we obtain that

$$\|[\tilde{\mathcal{P}}_T^l(\xi_h)\cdot\boldsymbol{t}]\|_{0,e}\leq h_e^{1/2}\sum_{T\in\omega_e}\left(h_T^{-1}\|\tilde{\mathcal{P}}_T^l(\xi_h)-\xi\|_{0,T}+\|\,\mathrm{rot}\,\tilde{\mathcal{P}}_T^l(\xi_h)\|_{0,T}\right).$$

Therefore, using the fact that $h_e\leq h_T$, we deduce that

$$h_e^{1/2}\|[\tilde{\mathcal{P}}_T^l(\xi_h)\cdot\boldsymbol{t}]\|_{0,e}\leq\sum_{T\in\omega_e}\left(\|\tilde{\mathcal{P}}_T^l(\xi_h)-\xi\|_{0,T}+h_T\|\,\mathrm{rot}\,\tilde{\mathcal{P}}_T^l(\xi_h)\|_{0,T}\right).$$

Now, repeating the arguments used in the proof of Lemma 4.10 allows us to prove that

$$\|\,\mathrm{rot}\,\tilde{\mathcal{P}}_T^l(\xi_h)\|_{0,T}\leq h_T^{-1}\|\tilde{\mathcal{P}}_T^l(\xi_h)-\xi\|_{0,T}.$$

From the above inequality and the Cauchy-Schwarz inequality, we obtain that

$$h_e^{1/2}\|[\tilde{\mathcal{P}}_T^l(\xi_h)\cdot\boldsymbol{t}]\|_{0,e}\leq C\sum_{T\in\omega_e}\left(\|\boldsymbol{f}-\tilde{\mathcal{P}}_T^l(\boldsymbol{f})\|_{0,T}+\|\boldsymbol{u}-\boldsymbol{u}_h\|_{0,T}+|\omega-\omega_h|_{1,T}\right). \tag{4.15}$$

Thus, the proof follows combining (4.13), (4.14), and (4.15). □

We end this section by observing that the required efficiency of the a posteriori error estimator $\boldsymbol{\theta}$ follows straightforwardly from Lemmas 4.8–4.12. In fact, from the estimates previously proved, we have that there exists $C>0$, independent of h, such that

$$\begin{aligned}\boldsymbol{\theta}^2\leq&C\Big(\|\boldsymbol{u}-\boldsymbol{u}_h\|_{\mathrm{H}(\mathrm{div};\Omega)}^2+\|\omega-\omega_h\|_{1,\Omega}^2+\|p-p_h\|_{0,\Omega}^2\\ &+\sum_{T\in\mathcal{T}_h}\|\boldsymbol{f}-\mathcal{P}_T^l(\boldsymbol{f})\|_{0,T}^2+h_T^2|\boldsymbol{f}-\mathcal{P}_T^l(\boldsymbol{f})|_{1,T}^2+\|\boldsymbol{f}-\tilde{\mathcal{P}}_T^l(\boldsymbol{f})\|_{0,T}^2+h_T^2|\boldsymbol{f}-\tilde{\mathcal{P}}_T^l(\boldsymbol{f})|_{1,T}^2\Big).\end{aligned} \tag{4.16}$$

In particular, if $\boldsymbol{f}\in\mathrm{H}^{k+2}(T)$ and $\mathcal{P}_T^l$ is the $L^2(T)^2$-orthogonal projection onto $\mathbb{P}_{k+2}(T)^2$ with respect to the inner product $(\boldsymbol{f},\boldsymbol{g})_{0,T}:=\int_T\psi_T\boldsymbol{f}\cdot\boldsymbol{g}$, and $\tilde{\mathcal{P}}_T^l$ is the $L^2(T)^2$-orthogonal projection onto $\mathbb{P}_{k+2}(T)^2$,

d.o.f.	h	$E_0(\omega)$	$r_0(\omega)$	$E_1(\omega)$	$r_1(\omega)$	$E_{\mathrm{div}}(\boldsymbol{u})$	$r_{\mathrm{div}}(\boldsymbol{u})$	$E_0(p)$	$r_0(p)$	$\Vert \operatorname{div} \boldsymbol{u}_h \Vert_{\infty,\Omega}$
Error history for $\mathbb{RT}_0 - \mathbb{P}_1 - \mathbb{P}_0$ approximations ($k = 0$)										
11	1.414210	11.71581	–	79.36864	–	2.805273	–	0.123333	–	5.1102e-27
33	0.707107	9.079022	0.567814	49.24973	0.722211	1.469431	0.867701	0.076084	1.075232	2.2131e-15
125	0.372678	4.895721	1.805791	36.23610	0.824171	1.020322	0.947812	0.042443	1.052781	6.7533e-15
195	0.306413	2.874370	2.028712	20.53772	1.038167	0.797743	0.985694	0.032645	1.034051	1.5987e-14
377	0.209106	1.254812	2.169230	13.68914	1.061382	0.545218	0.996092	0.022321	0.994946	4.8650e-14
885	0.150804	0.483292	2.191278	11.45945	1.037985	0.348818	1.036646	0.015658	1.084620	1.4766e-13
2639	0.082321	0.140461	2.041215	8.882926	0.976387	0.198771	0.992038	0.008948	0.984372	7.6457e-13
8787	0.047282	0.040224	2.055271	6.447363	1.102680	0.107771	1.103972	0.004926	1.076262	1.5495e-12
31541	0.024338	0.010076	2.084392	3.246562	1.033130	0.056278	0.978352	0.002623	0.984965	5.4851e-12
122475	0.013753	0.002831	2.022390	1.727322	1.105581	0.028899	1.016772	0.001545	0.972096	9.6870e-12
476513	0.007763	0.000713	2.041003	0.868747	1.201732	0.014508	1.020494	0.002599	0.988879	4.9247e-11
Error history for $\mathbb{RT}_1 - \mathbb{P}_2 - \mathbb{P}_1$(discontinuous) approximations ($k = 1$)										
29	1.414210	10.71021	–	55.46051	–	2.037612	–	0.044486	–	3.6134e-28
97	0.707107	2.376331	3.188072	32.19202	2.080623	0.895791	1.966108	0.020398	1.988557	3.5235e-17
393	0.372678	0.712077	3.387651	16.12852	1.928753	0.411085	1.924872	0.010371	2.087680	2.8592e-16
621	0.306413	0.155729	3.144132	6.016351	2.039671	0.153451	2.038251	0.003096	2.049997	5.6619e-16
1217	0.209106	0.052192	2.976262	2.901182	1.981934	0.072364	1.828472	0.001408	2.061082	2.1497e-15
2889	0.150804	0.017405	3.098324	1.429783	2.049258	0.033341	2.076681	0.000688	2.067212	1.7752e-14
8693	0.082321	0.002683	2.961543	0.430254	1.982384	0.010482	1.970886	0.000191	1.985533	5.2005e-14
29101	0.047282	0.000471	3.026058	0.139511	2.016524	0.003289	2.024584	0.000093	2.015291	1.4202e-13
104777	0.024338	7.0612e-5	2.986333	0.035421	1.952289	0.000863	2.014372	0.000047	2.021748	6.4270e-13
407549	0.013753	9.7511e-6	3.052339	0.009493	2.030695	0.000239	2.024462	0.000024	2.186360	1.7082e-12
1586993	0.007763	2.4283e-6	2.997468	0.002379	2.019762	0.000062	2.017938	0.000017	2.038975	3.9629e-12

TABLE 1. Test 1: Convergence history for the mixed $\mathbb{RT}_0 - \mathbb{P}_1 - \mathbb{P}_0$ (top rows) and $\mathbb{RT}_1 - \mathbb{P}_2 - \mathbb{P}_1$ (bottom rows) FE approximations of velocity-vorticity-pressure according to the Bercovier-Engelman test, on a sequence of non-uniformly refined triangulations of the unit square.

for each $T \in \mathcal{T}_h$, we obtain

$$\sum_{T\in\mathcal{T}_h} \|\boldsymbol{f}-\mathcal{P}_T^{k+2}(\boldsymbol{f})\|_{0,T}^2 + h_T^2|\boldsymbol{f}-\mathcal{P}_T^{k+2}(\boldsymbol{f})|_{1,T}^2 + \|\boldsymbol{f}-\tilde{\mathcal{P}}_T^{l}(\boldsymbol{f})\|_{0,T}^2 + h_T^2|\boldsymbol{f}-\tilde{\mathcal{P}}_T^{l}(\boldsymbol{f})|_{1,T}^2 \leq Ch^{2(k+2)} \sum_{T\in\mathcal{T}_h} \|\boldsymbol{f}\|_{k+2,T}^2,$$

which corresponds to a higher order term. This inequality and (4.16) complete the proof of Theorem 4.2.

5. Numerical results

In what follows, we present four numerical examples illustrating the performance of the FE methods described in Section 3, and which confirm the theoretical error bounds. Individual errors are denoted by

$$E_0(\omega) := \|\omega - \omega_h\|_{0,\Omega},\ E_1(\omega) := \|\omega - \omega_h\|_{1,\Omega},\ E_{\mathrm{div}}(\boldsymbol{u}) := \|\boldsymbol{u} - \boldsymbol{u}_h\|_{\mathrm{H(div;\Omega)}},\ E_0(p) := \|p - p_h\|_{0,\Omega}.$$

In the numerical tests, we study the accuracy of the discretization by observing these errors on successively refined non-uniform partitions of Ω. Convergence rates are defined as usual

$$r(\cdot) := \frac{\log(E(\cdot)/\hat{E}(\cdot))}{\log(h/\hat{h})}, \tag{5.1}$$

where E and $\hat{E}$ denote errors associated to two consecutive meshes of sizes h and $\hat{h}$. The linear systems arising from the discrete formulations (3.4),(3.19) have been solved using the multifrontal massively parallel sparse direct solver MUMPS [4].

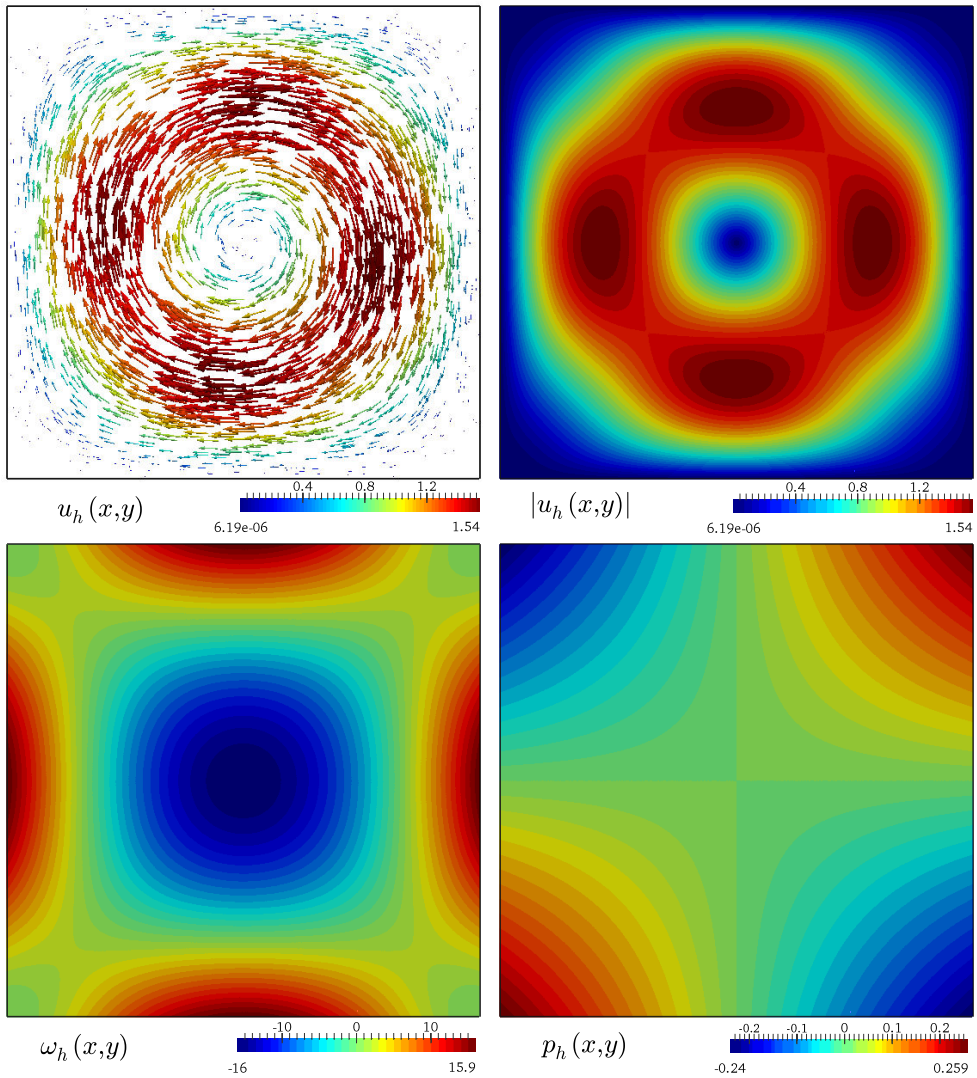

FIGURE 1. Test 1: Approximated velocity field and velocity magnitude (top), vorticity (bottom left), and computed pressure (bottom right) with a $\mathbb{RT}_1-\mathbb{P}_2-\mathbb{P}_1$ family for the Bercovier-Engelman solutions to the generalized Stokes problem with $\sigma = 0.1$, computed on an unstructured mesh of 134162 elements and 67700 vertices.

5.1. **Test 1: Mesh convergence with respect to the Bercovier-Engelman solutions.** As numerical validation of the convergence properties of our method, we first consider $\Omega = (0,1)^2$, and $\Gamma = \partial\Omega$, $\nu = 0.01$, $\sigma = 0.1$, and choose the data $\boldsymbol{f}, \boldsymbol{b}, \omega_0$ so that the solution of the problem is given by the Bercovier-Engelman functions [9]

$$\omega(x,y) = 256[x^2(x-1)^2(6y^2-6y+1) + y^2(y-1)^2(6x^2-6x+1)],$$
$$\boldsymbol{u}(x,y) = \begin{pmatrix} -256x^2(x-1)^2y(y-1)(2y-1) \\ 256y^2(y-1)^2x(x-1)(2x-1) \end{pmatrix}, \quad p(x,y) = (x-1/2)(y-1/2),$$

which are smooth in Ω. Table 1 summarizes the convergence behavior of two mixed finite element families corresponding to $k = 0$ and $k = 1$. Both mixed methods associated to different polynomial degrees attain optimal rates of convergence of order $O(h^{k+1})$ for vorticity in the $\mathrm{H}^1(\Omega)-$norm, for velocity in the

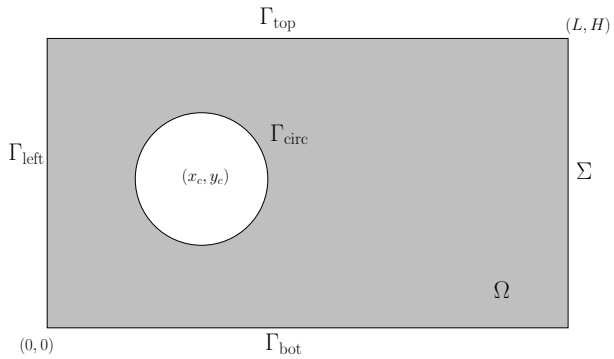

FIGURE 2. Test 2: Sketch of the geometry employed in the simulation of steady flow past a cylinder.

H(div; Ω)−norm, and for pressure in the $\mathrm{L}^2(\Omega)$−norm as predicted by the theory. In addition, we observe that the vorticity ω_h converges with order $O(h^{k+2})$ to ω in the $\mathrm{L}^2(\Omega)$-norm. The last column of Table 1 illustrates that the velocity is practically divergence free for all refinement steps, and for both $k = 0$ and $k = 1$. Approximate solutions computed with a $\mathbb{RT}_1 - \mathbb{P}_2 - \mathbb{P}_1$ family on a mesh of 134162 elements and 67700 vertices are provided in Figure 1.

5.2. **Test 2: Flow past a cylinder.** Our next example focuses on the simulation of steady channel flow around a cylinder and confined between two parallel plates. The radius of the cylinder is $R = 0.1$, and the length and height of the channel are $L = 0.82$, $H = 0.41$, respectively. The geometry and setting of the problem allows to consider the two-dimensional domain $\Omega = (0, L) \times (0, H) \setminus B_R(x_c, y_c)$, where $B_R(x_c, y_c)$ is the disk of radius R centered in $(x_c, y_c) = (0.2, 0.2)$ (see Figure 2). There we also sketch the boundaries, where we specify the following data. On Γ (left, top, bottom and "cylinder surface" boundaries) we set normal velocities and vorticity as

$$\boldsymbol{u} \cdot \boldsymbol{n} = \boldsymbol{b} \cdot \boldsymbol{n}, \text{ with } \boldsymbol{b}(x, y) = \begin{cases} \boldsymbol{0} & \text{on } \Gamma_{\text{circ}}, \\ \left(\dfrac{4u_{\max} y(H - y)}{H^2}, 0 \right)^{\mathtt{t}} & \text{on } \Gamma_{\text{top}}, \Gamma_{\text{bot}}, \Gamma_{\text{left}}, \end{cases}$$

$$\omega = \omega_0(x, y) = \operatorname{rot} \boldsymbol{b} = \begin{cases} 0 & \text{on } \Gamma_{\text{circ}}, \\ \dfrac{-4u_{\max}(H - 2y)}{H^2} & \text{on } \Gamma_{\text{top}}, \Gamma_{\text{bot}}, \Gamma_{\text{left}}, \end{cases}$$

and on Σ (right boundary) we set zero tangential velocities and zero pressure

$$\boldsymbol{u} \cdot \boldsymbol{t} = \boldsymbol{a} \cdot \boldsymbol{t} = 0, \text{ with } \boldsymbol{a}(x, y) = \left(\frac{4u_{\max} y(H - y)}{H^2}, 0 \right)^{\mathtt{t}}, \quad p = p_0(x, y) = 0.$$

We choose $u_{\max} = 1.5$, $\nu = 1e - 4$, $\sigma = 0.01$ and the approximate solutions obtained on a triangular mesh of 157798 elements and 79499 vertices (representing 474594 degrees of freedom for the lowest order $\mathbb{RT}_0 - \mathbb{P}_1 - \mathbb{P}_0$ family of finite elements) are presented in Figure 3. In the lack of a known exact solution, we compute the L^∞−norm of the velocity, and errors in different norms and on successively refined grids, with respect to a reference solution obtained on a highly refined mesh. These are reported in Table 2.

5.3. **Test 3: The lid-driven cavity flow.** In this example, we perform the classical lid-driven cavity test where we model the steady flow of an immiscible fluid in a box. The domain is again the unit square $\Omega = (0, 1)^2$ and we consider an unstructured mesh with 81738 elements. We first fix $\sigma = 1e-4$, $\nu = 0.001$, and take Γ as the bottom, right, and left boundaries, and Σ is the top lid of the domain. In this test the boundary conditions are not covered by the present analysis: on Γ we set $\boldsymbol{u} \cdot \boldsymbol{n} = 0$, whereas on Σ we set $\boldsymbol{u} \cdot \boldsymbol{t} = 1$, however the approximate velocities, pressure and vorticity (displayed in Figure 4) remain

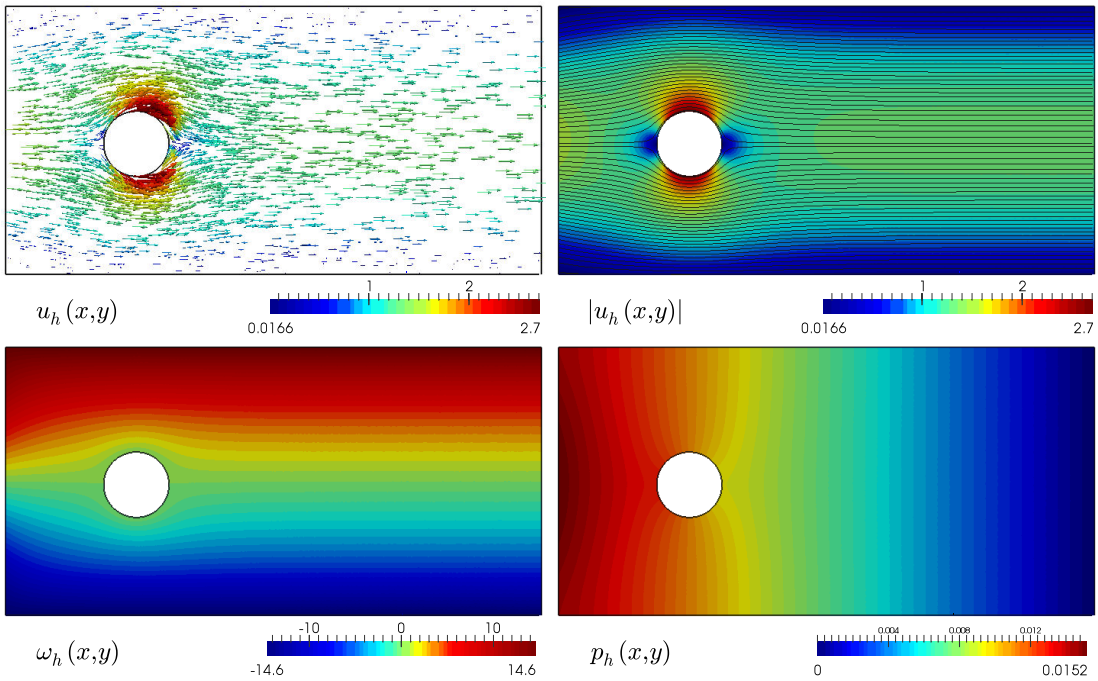

FIGURE 3. Test 2: Approximated velocity field and velocity magnitude (top), vorticity (bottom left), and computed pressure (bottom right) with a $\mathbb{RT}_0 - \mathbb{P}_1 - \mathbb{P}_0$ family for the steady flow past a cylinder.

d.o.f.	h	$E_0(\omega_{\rm ref})$	$r_0(\omega_{\rm ref})$	$E_1(\omega_{\rm ref})$	$r_1(\omega_{\rm ref})$	$E_{\rm div}(\boldsymbol{u}_{\rm ref})$	$r_{\rm div}(\boldsymbol{u}_{\rm ref})$	$E_0(p_{\rm ref})$	$r_0(p_{\rm ref})$	$\Vert \operatorname{div} \boldsymbol{u}_h \Vert_{\infty,\Omega}$
102	0.412471	2.534604	–	90.8724	–	0.150189	–	0.004289	–	7.8515e-16
378	0.205287	1.172105	1.10578	46.6781	0.88291	0.082220	0.86979	0.002362	0.96363	2.0680e-15
1248	0.109821	0.429278	1.65721	30.2369	0.75982	0.045807	0.93719	0.000772	1.79086	3.3116e-15
4836	0.067933	0.113782	2.61802	15.6170	1.21681	0.023889	1.35533	0.000369	1.53259	6.5773e-15
19200	0.036926	0.032748	2.09970	7.98976	1.04287	0.012533	1.05819	0.000181	1.17699	1.3601e-14
76050	0.019449	0.007355	2.18462	4.25320	0.95921	0.006385	1.05183	9.2412e-5	1.02422	2.6869e-14
302298	0.009285	0.001519	2.13157	2.67387	0.82396	0.003643	0.75879	5.1767e-5	0.77454	5.3728e-14

TABLE 2. Test 2: Experimental convergence of the mixed $\mathbb{RT}_0 - \mathbb{P}_1 - \mathbb{P}_0$ FE approximation of the steady flow around a cylinder with respect to a reference solution $(\boldsymbol{u}_{\rm ref}, \omega_{\rm ref}, p_{\rm ref})$ computed on a highly refined grid.

stable and corner singularities are well resolved. Moreover, to assess the robustness of the method with respect to the choice of σ, we run several tests keeping fixed $\nu = 0.001$ and varying σ over several orders of magnitude. Plots of streamlines for each case are depicted in Figure 5, confirming the stability of the approximations in all cases.

5.4. **Test 4: Flow into a backwards facing step.** Another classical benchmark test for Stokes and Navier-Stokes problems is the backwards facing step. In this example, the geometry consists on a channel of total height $2H$ and length $9H$, with a backwards facing step of height is $H = 1$, where the reentrant corner is located at (H, H). No external forces are applied, whereas boundary data are set as follows: At the inlet region (left boundary) we impose a Poiseuille inflow (normal) velocity $\boldsymbol{u}\cdot\boldsymbol{n} = u_{\max} - \frac{1}{2}(y - \frac{3}{2}H)^2$ and a compatible vorticity $\omega_0 = y - \frac{3}{2}H$, where the maximum speed of the inflow is $u_{\max} = 0.125$. At the

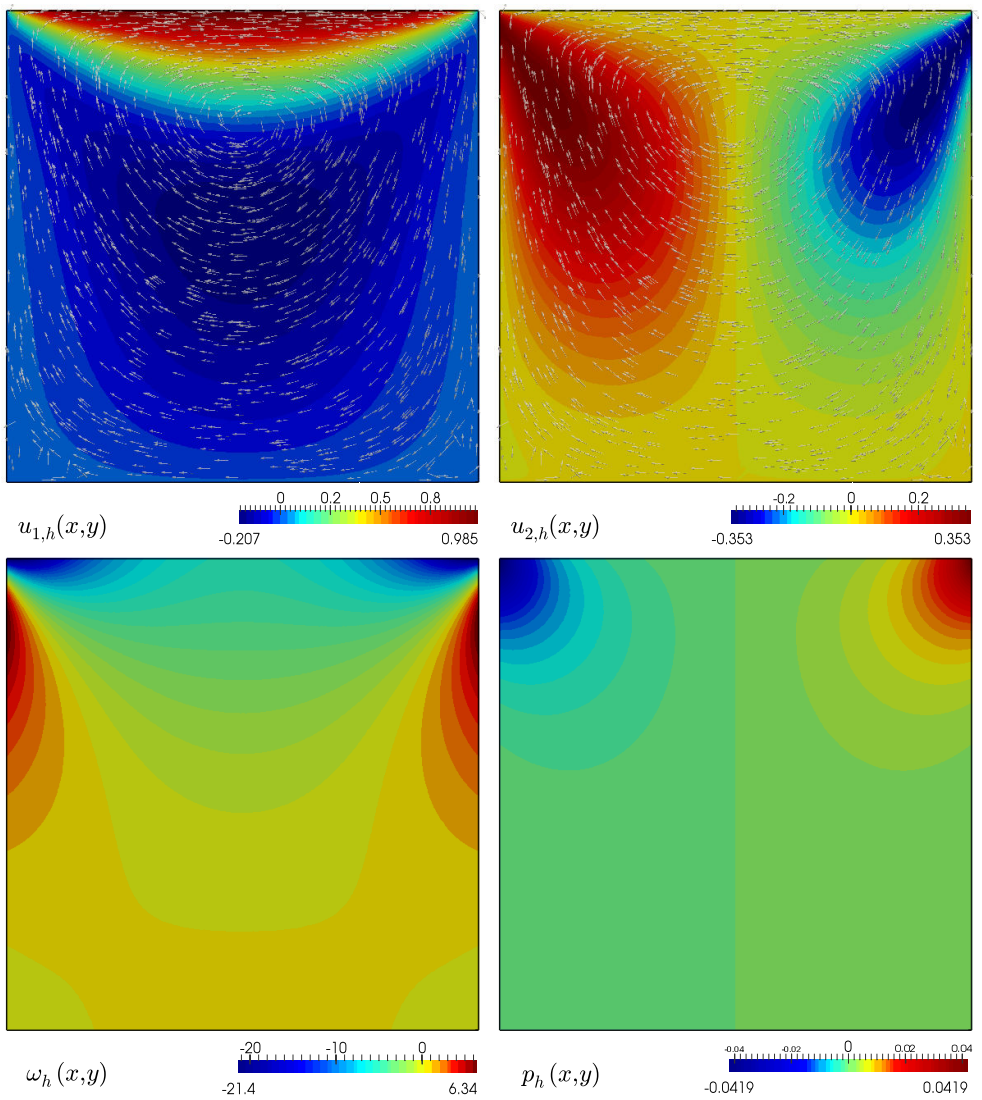

FIGURE 4. Test 3: Approximated velocity components (top), vorticity (bottom left), and computed pressure (bottom right) with a $\mathbb{RT}_0 - \mathbb{P}_1 - \mathbb{P}_0$ family for the lid-driven cavity test.

outlet (right face) we apply a constant pressure $p_0 = 0$, and on the remaining segments conforming $\partial\Omega$ we impose slip velocity conditions ($\boldsymbol{u} \cdot \boldsymbol{n} = 0$) and zero vorticity $\omega_0 = 0$. We generate an unstructured mesh consisting of 226462 triangles and 113202 vertices, and the model parameters are chosen to be $\sigma = \nu = 0.0001$. Approximate solutions obtained with a $\mathbb{BDM}_1 - \mathbb{P}_2 - \mathbb{P}_0$ family are reported in Figure 6, where some expected phenomena well-documented in the literature (including corner singularities, fluid recirculation zone, and vortex generation), can be observed.

5.5. **Test 5: A posteriori error estimation.** We close this section by numerically testing the efficiency of the a posteriori error estimator (4.1) and applying mesh refinement according to the local value of the

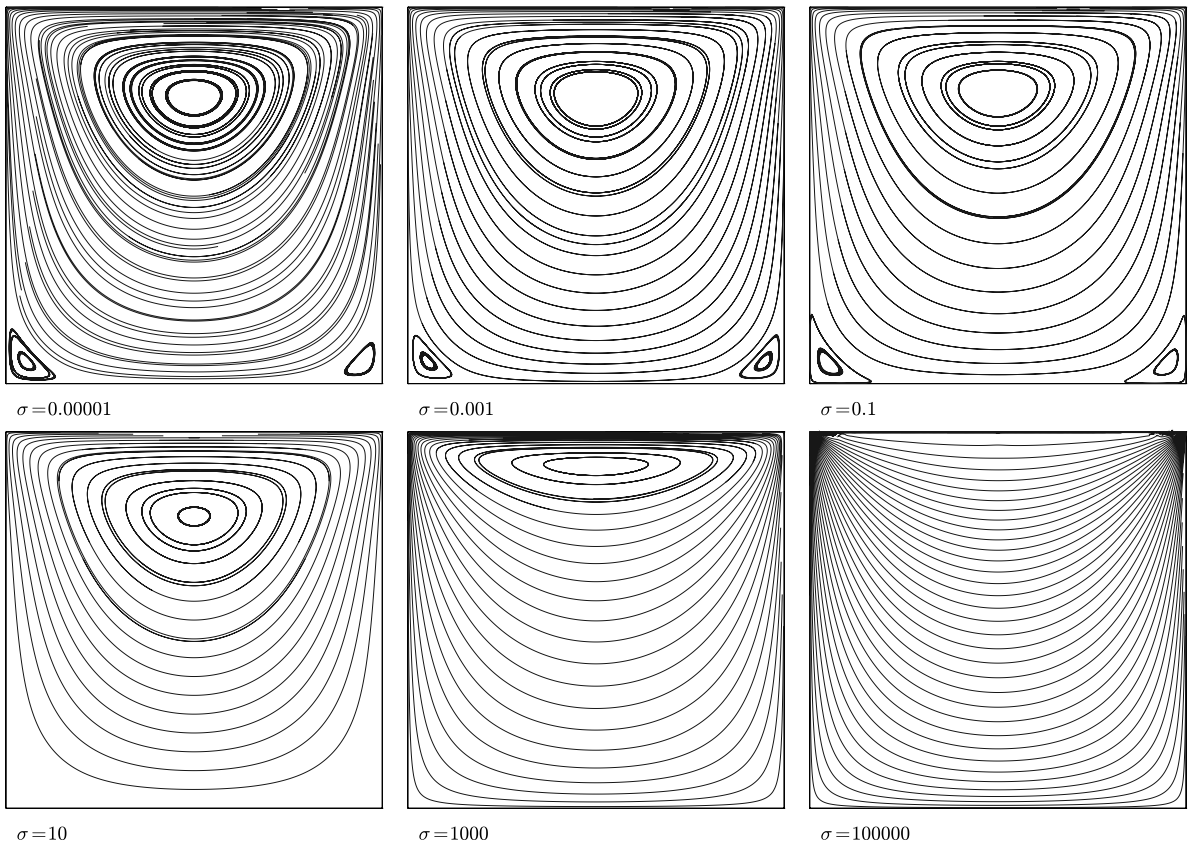

FIGURE 5. Test 3: Computed streamlines for different values of σ, obtained with a $\mathbb{RT}_0 - \mathbb{P}_1 - \mathbb{P}_0$ approximation of the lid-driven cavity test.

indicator. In this case the convergence rates are no longer defined as in (5.1), but we consider instead

$$r(\cdot) := \frac{\log(E(\cdot)/\hat{E}(\cdot))}{-\frac{1}{2}\log(N/\hat{N})},$$

where N and $\hat{N}$ denote the corresponding degrees of freedom at each triangulation. We recall the definition of the so-called effectivity index as the ratio between the total error and the global error estimator, i.e.,

$$\mathtt{e} := \left\{[E_{\mathrm{div}}(\boldsymbol{u})]^2 + [E_1(\omega)]^2 + [E_0(p)]^2\right\}^{1/2}, \quad \mathtt{r} := \frac{\log(\mathtt{e}/\hat{\mathtt{e}})}{-\frac{1}{2}\log(N/\hat{N})}, \quad \mathtt{eff} := \frac{\mathtt{e}}{\boldsymbol{\theta}}.$$

Here we employ $\mathbb{RT}_0$ approximations for velocities, piecewise linear elements for vorticity, and piecewise constant approximations for the pressure field. The computational domain is the nonconvex L-shaped domain $\Omega = (-1,1)^2 \setminus (0,1)^2$, where problem (1.1) admits the following exact solution

$$\boldsymbol{u}(x,y) = \begin{pmatrix} -\pi\sin(\pi x)\cos(\pi y) \\ \pi\cos(\pi x)\sin(\pi y) \end{pmatrix}, \quad \omega(x,y) = -2\pi^2\sin(\pi y)\sin(\pi x),$$
$$p(x,y) = \frac{1-x^2-y^2}{(x-c)^2+(y-c)^2} - \int_\Omega \frac{1-x^2-y^2}{(x-c)^2+(y-c)^2}\,\mathrm{d}x\,\mathrm{d}y,$$

satisfying $\boldsymbol{u}\cdot\boldsymbol{n} = 0$ and $\omega = \omega_0 = 0$ on $\Gamma = \partial\Omega$ (and therefore falling into the framework where the a posteriori error analysis of Section 4 is valid). Model parameters are set to $\sigma = 0.1$, $\nu = 0.01$, $c = 0.05$ and

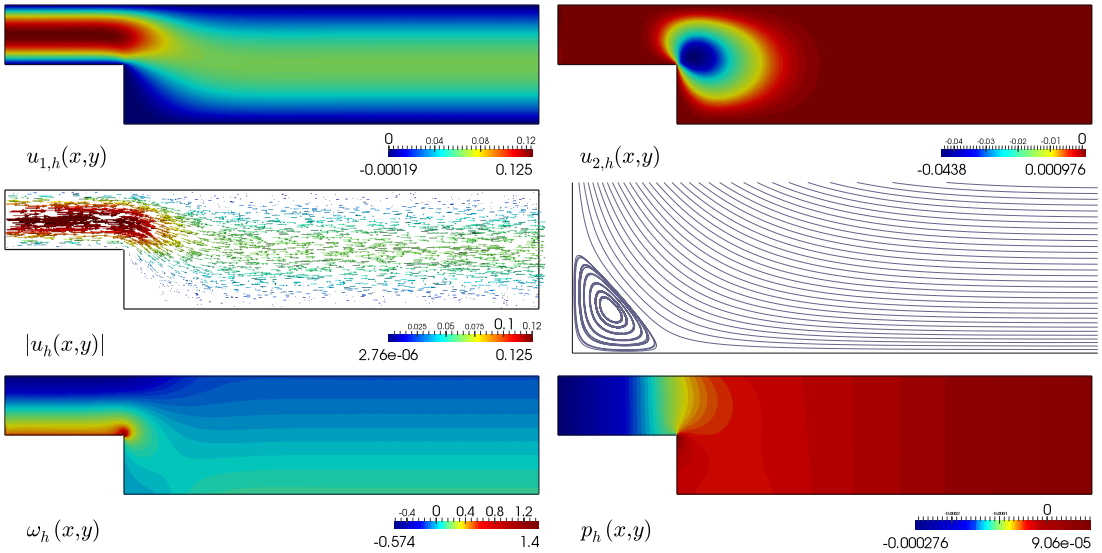

FIGURE 6. Test 4: Velocity components (top panels), velocity vectors (middle left), zoomed velocity streamlines on the left bottom part of the channel (middle right panel), vorticity (bottom left) and pressure distribution (bottom right), computed with a $\mathbb{BDM}_1 - \mathbb{P}_2 - \mathbb{P}_0$ approximation for a generalized Stokes flow into a backwards facing step.

we notice that the pressure is singular near the reentrant corner of the domain and so we expect hindered convergence of the approximations when a uniform (or quasi-uniform) mesh refinement is applied. Such a degeneracy of the optimal convergence rates is indeed observed from the first rows in Table 3. In contrast, if we apply a classical adaptive mesh refinement procedure (here based on an equi-distribution of the discrete error indicators, where the diameter of each element in $\mathcal{T}_{h_{i+1}}$, which is contained in a generic element $T \in \mathcal{T}_{h_i}$ in the new step of the algorithm, is proportional to the diameter of T times the ratio $\hat{\boldsymbol{\theta}}_T/\boldsymbol{\theta}_T$, where $\hat{\boldsymbol{\theta}}_T$ is the mean value of the estimator over $\mathcal{T}_h$, see also [1, 22, 38]) from the bottom rows of Table 3 we observe a recovering of the optimal convergence rates as predicted by the theory and a more stable effectivity index associated to the global error indicator. The resulting meshes after a few adaptation steps are reported in Figure 7. We observe intensive refinement near the reentrant corner of the domain and a slight refinement near the zones of high vorticity and velocity gradients. Approximate solutions rendered on a fine mesh of 45789 triangles and 28765 vertices are presented in Figure 8, where we can observe well-resolved profiles for all fields.

6. Concluding remarks

In this work, we have presented a new mixed finite element method for the discretization of the vorticity-velocity-pressure formulation of the generalized Stokes equations. The key features of the proposed method are the liberty to choose different inf-sup stable finite element families, the direct and accurate access to vorticity without invoking any kind of postprocessing, the exactly divergence-free approximation of the velocity field, and a natural analysis in the framework of a generalized Babuška-Brezzi theory. We consider these capabilities as of great interest and foresee the application of the same framework in the study of several extensions, including the three-dimensional case and the coupling with Darcy flow and with transport phenomena. An a posteriori error analysis has been carried out, and some numerical tests have been presented to confirm the theoretically predicted decay of the error, and to illustrate the robustness, reliability and efficiency of the proposed method.

N	h	$E_0(\omega)$	$r_0(\omega)$	$E_{\rm div}(\boldsymbol{u})$	$r_{\rm div}(\boldsymbol{u})$	$E_0(p)$	$r_0(p)$	$\Vert \operatorname{div} \boldsymbol{u}_h \Vert_{\infty,\Omega}$	e	r	eff
					Quasi-uniform refinement						
27	1.414210	74.91495	–	9.468466	–	19.26487	–	1.2860e-13	95.57550	–	0.031999
89	0.750102	71.11422	0.130916	7.180972	0.282924	15.14127	0.823585	1.6506e-12	91.15603	0.229817	0.234602
345	0.400195	67.17051	0.106407	6.307011	0.545829	13.43716	0.176243	6.3785e-12	87.65119	0.165055	0.205222
1385	0.190086	45.11124	0.444451	2.331924	1.431725	11.37382	0.239883	1.2310e-11	75.44525	0.244415	0.200572
5319	0.102545	18.27292	2.551982	0.339012	2.866262	7.373953	0.644122	1.8359e-11	39.57076	1.410870	0.015233
20939	0.050658	3.296340	2.499561	0.155864	1.134111	3.769263	0.979438	2.7667e-11	15.00973	0.899889	0.004698
83439	0.027321	1.847672	0.789376	0.078403	0.994027	2.208534	0.773316	3.2138e-11	3.697965	0.895531	0.002178
333761	0.013899	1.070631	0.800598	0.039041	1.005880	1.594542	0.621276	3.5752e-11	2.339175	0.701805	0.001120
					Adaptive refinement						
27	1.414210	74.91491	–	9.468466	–	19.26488	–	1.2881e-13	95.57551	–	0.858014
101	0.719555	65.14843	0.703912	6.459844	1.074953	16.02282	0.830424	1.2702e-12	86.17032	0.693521	0.906312
299	0.578902	47.02231	0.461757	4.725962	1.083581	11.42728	0.622914	1.0250e-11	73.12423	0.464138	0.916647
539	0.500000	31.10482	1.501281	1.430722	2.055545	7.787812	1.301350	1.9323e-11	41.71467	1.463174	0.896883
1109	0.362583	19.28521	1.701442	0.985249	1.034061	3.758322	2.019651	2.8919e-11	19.67272	1.679176	0.887776
4375	0.179643	9.346472	1.055548	0.474551	1.064565	1.814664	1.060982	3.5205e-11	9.532834	1.055768	0.913295
25953	0.111922	3.748725	1.026291	0.189981	1.028372	0.690889	1.084839	3.7586e-11	3.816574	1.028315	0.902185
180903	0.042313	1.400535	1.014143	0.070955	1.014457	0.269499	0.969693	4.8971e-11	1.427993	1.012623	0.903122

TABLE 3. Test 5: Convergence history for the mixed $\mathbb{RT}_0 - \mathbb{P}_1 - \mathbb{P}_0$ FE approximations of velocity-vorticity-pressure computed on a sequence of quasi-uniformly (top rows) and adaptively (bottom rows) refined triangulations of the L-shaped domain.

ACKNOWLEDGEMENTS

V. Anaya was partially supported by CONICYT-Chile through FONDECYT postdoctorado No.3120197, by project Inserción de Capital Humano Avanzado en la Academia No. 79112012, and DIUBB through project 120808 GI/EF. D. Mora was partially supported by CONICYT-Chile through FONDECYT project No.1140791, by DIUBB through project 120808 GI/EF, and Anillo ANANUM, ACT1118, CONICYT (Chile). R. Oyarzúa was partially supported by CONICYT-Chile through FONDECYT project No.1121347, by DIUBB through project 120808 GI/EF, and Anillo ANANUM, ACT1118, CONICYT (Chile). This work was advanced during a visit of V. Anaya and D. Mora to the Institut des Sciences de la Terre, University of Lausanne.

REFERENCES

[1] M. AINSWORTH AND J. ODEN, *A posteriori error estimation in finite element analysis*. Pure and Applied Mathematics. Wiley, New York (2000).

[2] M. AMARA, D. CAPATINA-PAPAGHIUC, AND D. TRUJILLO, *Stabilized finite element method for Navier-Stokes equations with physical boundary conditions*. Math. Comp., 76(259) (2007) 1195–1217.

[3] M. AMARA, E. CHACÓN VERA, AND D. TRUJILLO, *Vorticity–velocity–pressure formulation for Stokes problem*. Math. Comp., 73(248) (2004) 1673–1697.

[4] P.R. AMESTOY, I.S. DUFF, AND J.Y. L'EXCELLENT, *Multifrontal parallel distributed symmetric and unsymmetric solvers*. Comput. Methods Appl. Mech. Engrg., 184(2-4) (2000) 501–520.

[5] V. ANAYA, D. MORA, G.N. GATICA, AND R. RUIZ-BAIER, *An augmented velocity-vorticity-pressure formulation for the Brinkman problem*. CI^{2}MA preprint 2014-11, available from `http://www.ci2ma.udec.cl/publicaciones/prepublicaciones`.

[6] V. ANAYA, D. MORA, C. REALES, AND R. RUIZ-BAIER, *Stabilized mixed finite element approximation of axisymmetric Brinkman flows*. CI^{2}MA preprint 2014-19, available from `http://www.ci2ma.udec.cl/publicaciones/prepublicaciones`.

[7] V. ANAYA, D. MORA, AND R. RUIZ-BAIER, *An augmented mixed finite element method for the vorticity-velocity-pressure formulation of the Stokes equations*. Comput. Methods Appl. Mech. Engrg., 267 (2013) 261–274.

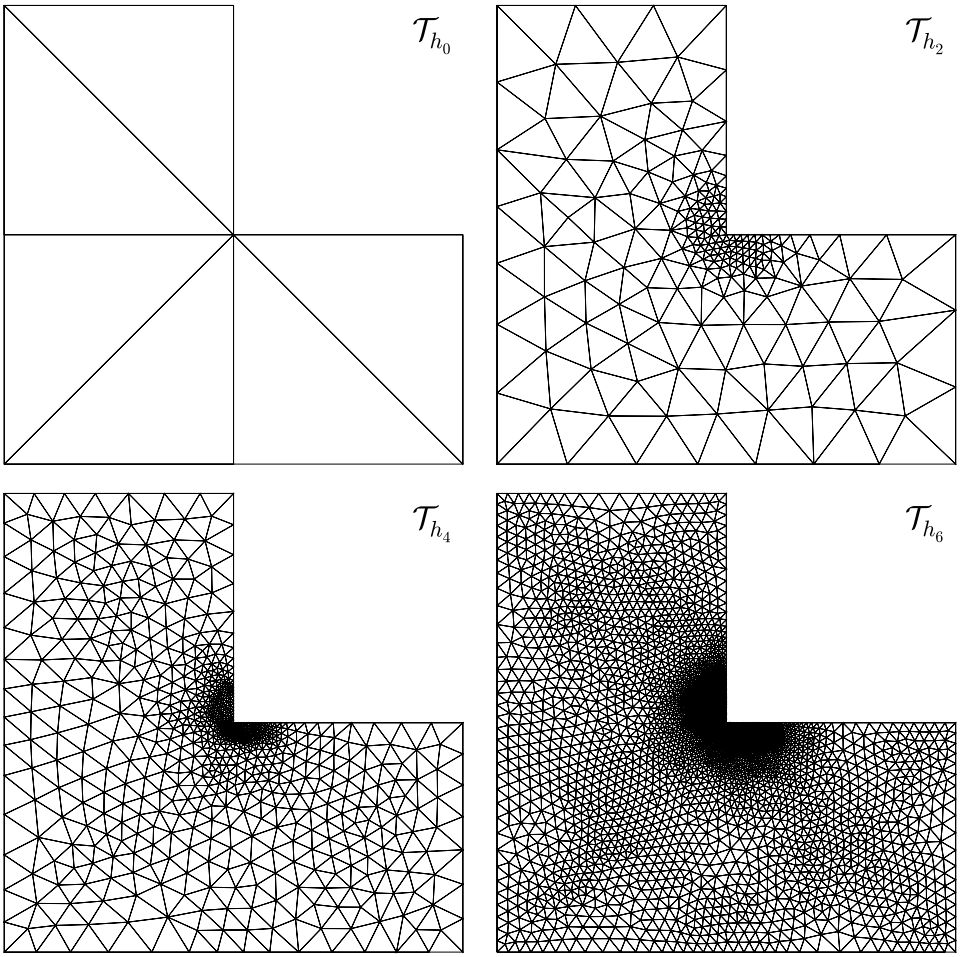

FIGURE 7. Test 5: Snapshots of four grids adaptively refined according to the a posteriori error indicator defined in (4.1).

[8] I. Babuška and G.N. Gatica, *A residual-based a posteriori error estimator for the Stokes-Darcy coupled problem*. SIAM J. Numer. Anal., 48(2) (2010) 498–523.

[9] M. Bercovier, and M. Engelman, *A finite element for the numerical solution of viscous incompressible flows*. J. Comput. Phys., 30 (1979) 181–201.

[10] C. Bernardi, and N. Chorfi, *Spectral discretization of the vorticity, velocity, and pressure formulation of the Stokes problem*. SIAM J. Numer. Anal., 44(2) (2007) 826–850.

[11] P.V. Bochev, *Analysis of least-squares finite element methods for the Navier–Stokes equations*. SIAM J. Numer. Anal., 34(5) (1997) 1817–1844.

[12] P.V. Bochev, and M. Gunzburger, *Least-Squares finite element methods*. Volume 166 of Applied Mathematical Sciences. Springer Verlag (2009).

[13] D. Boffi, F. Brezzi, and M. Fortin, *Mixed Finite Element Methods and applications*. Springer Series in Computational Mathematics, 44. Springer, Heidelberg (2013).

[14] R. Bustinza, G.N. Gatica, and M. González, *A mixed finite element method for the generalized Stokes problem*. Int. J. Numer. Methods Fluids, 49(8) (2005) 877–903.

[15] C. Carstensen, *A posteriori error estimate for the mixed finite element method*. Math. Comp., 66(218) (1997) 465–476.

[16] C.L. Chang, *A mixed finite element method for the Stokes problem: an acceleration-pressure formulation*. Appl. Math. Comput. 36(2), (1990) 135–146.

[17] C.L. Chang, and B.-N. Jiang, *An error analysis of least-squares finite element method of velocity-pressure-vorticity formulation for the Stokes problem*. Comput. Meth. Appl. Mech. Engrg., 84(3) (1990) 247–255.

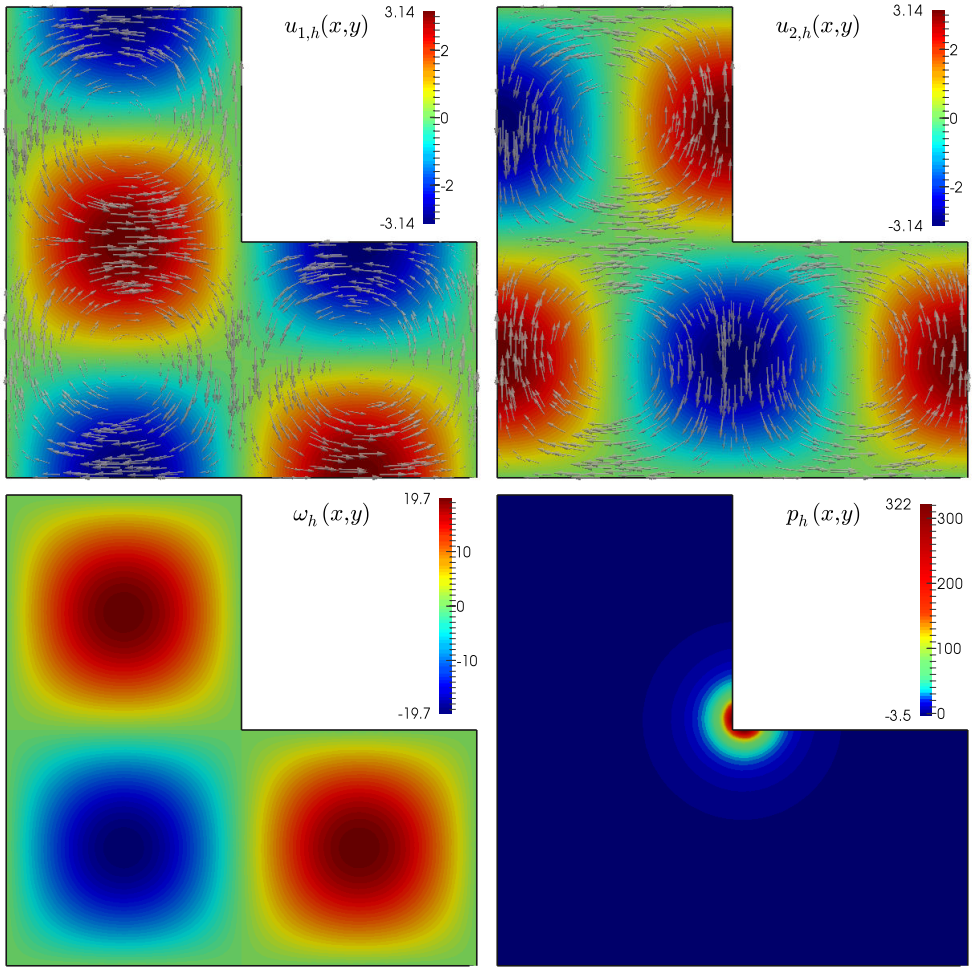

FIGURE 8. Test 5: Approximated velocity components (top), vorticity (bottom left), and computed pressure (bottom right) with a $\mathbb{RT}_0 - \mathbb{P}_1 - \mathbb{P}_0$ family on an adaptive mesh for the L-shaped domain.

[18] P. CLÉMENT, *Approximation by finite element functions using local regularisation*. RAIRO Modél. Math. Anal. Numér., 9 (1975) 77–84.

[19] B. COCKBURN, AND J. CUI, *An analysis of HDG methods for the vorticity-velocity-pressure formulation of the Stokes problem in three dimensions*. Math. Comp., 81(279) (2012) 1355–1368.

[20] H.-Y. DUAN, AND G.-P. LIANG, *On the velocity-pressure-vorticity least-squares mixed finite element method for the 3D Stokes equations*. SIAM J. Numer. Anal., 41(6) (2003) 2114–2130.

[21] F. DUBOIS, M. SALAÜN, AND S. SALMON, *First vorticity-velocity-pressure numerical scheme for the Stokes problem*. Comput. Methods Appl. Mech. Engrg., 192(44–46) (2003) 4877–4907.

[22] P.J. FREY, AND P.-L. GEORGE, *Maillages, applications aux éléments finis*. Hermès, Paris (1999).

[23] G.N. GATICA, *A Simple Introduction to the Mixed Finite Element Method. Theory and Applications*. Springer Briefs in Mathematics, Springer, Cham Heidelberg New York Dordrecht London (2014).

[24] G.N. GATICA, L.F. GATICA, AND A. MÁRQUEZ, *Augmented mixed finite element methods for a vorticity-based velocity–pressure–stress formulation of the Stokes problem in 2D*. Int. J. Numer. Methods Fluids, 67(4) (2011) 450–477.

[25] G.N. GATICA, L.F. GATICA, AND A. MÁRQUEZ, *Analysis of a pseudostress-based mixed finite element method for the Brinkman model of porous media flow*. Numer. Math., 126(4) (2014) 635–677.

[26] G.N. GATICA, N. HEUER, AND S. MEDDAHI, *On the numerical analysis of nonlinear twofold saddle point problems*. IMA J. Numer. Anal., 23(2) (2003) 301–330.

[27] G.N. GATICA, R. OYARZÚA, AND F.-J. SAYAS, *Analysis of fully-mixed finite element methods for the Stokes-Darcy coupled problem*. Math. Comp., 80(276) (2011) 1911–1948.

[28] G.N. Gatica, R. Oyarzúa, and F.J. Sayas, *A residual-based a posteriori error estimator for a fully-mixed formulation of the Stokes-Darcy coupled problem*. Comput. Methods Appl. Mech. Engrg., 200(21-22) (2011) 1877–1891.

[29] V. Girault, *Incompressible finite element methods for Navier-Stokes equations with non-standard boundary conditions in* $\mathbb{R}^3$. Math. Comp., 51(183) (1988) 55–74.

[30] V. Girault, and P. A. Raviart, *Finite element methods for Navier-Stokes equations. Theory and algorithms*. Springer-Verlag, Berlin (1986).

[31] J. S. Howell, *Approximation of generalized Stokes problems using dual-mixed finite elements without enrichment*. Int. J. Numer. Methods Fluids, 67(2) (2011) 247–268.

[32] K.H. Karlsen, and T. K. Karper, *Convergence of a mixed method for a semi-stationary compressible Stokes system*. Math. Comp., 80 (2011) 1459–1498.

[33] J.P. Pontaza, and J.N. Reddy, *Spectral/hp least-squares finite element formulation for the Navier-Stokes equations*. J. Comput. Phys., 190(2) (2003) 523–549.

[34] M. Salaün, and S. Salmon, *Numerical stabilization of the Stokes problem in vorticity-velocity-pressure formulation*. Comput. Methods Appl. Mech. Engrg., 196(9-12) (2007) 1767–1786.

[35] M. Salaün, and S. Salmon, *Low-order finite element method for the well-posed bidimensional Stokes problem*. IMA J. Numer. Anal., doi:10.1093/imanum/drt063 (in press 2014).

[36] C.G. Speziale, *On the advantages of the vorticity-velocity formulations of the equations of fluid dynamics*. J. Comput. Phys., 73(2) (1987) 476–480.

[37] P.S. Vassilevski, and U. Villa, *A mixed formulation for the Brinkman problem*. SIAM J. Numer. Anal., 52(1) (2014) 258–281.

[38] R. Verfürth, *A review of a posteriori error estimation and adaptive-mesh-refinement techniques*. Wiley-Teubner, Chichester (1996).